HANDSHAKE PROTOCOLS FOR ENERGY HARVESTING COMMUNICATIONS

by

Onur Tatar

B.S., Electrical & Electronics Engineering, Boğaziçi University, 2021

Submitted to the Institute for Graduate Studies in
Science and Engineering in partial fulfillment of
the requirements for the degree of
Master of Science

Graduate Program in Electrical & Electronics Engineering
Boğaziçi University
2024

ACKNOWLEDGEMENTS

Completing my master's degree has been an enriching and vibrant journey, one that would have been far less rewarding without several key individuals.

Foremost, I extend my deepest gratitude to Professors Hakan Deliç and Mutlu Koca. Their unwavering sincerity, mentorship, wisdom, patience, support, and guidance have been the cornerstone of my academic journey. Their influence has transformed what could have been a dull and unfruitful endeavor into an exciting and productive experience. I am also immensely grateful to Professor Emin Anarım for his belief in me, which bolstered my confidence and determination to persevere through my Master's program. His support has been a beacon of motivation, guiding me through challenging times. In addition, I would like to thank Professor Hakan Ali Çırpan for being on my thesis committee and his comments.

A special thank you goes to my darling, Müge Şenay. Her companionship during the best moments and her unrelenting support during the most stressful periods have been invaluable. She has been sharing the burdens and joys of this journey.

I am equally thankful to my lab mates, Ramazan Yılmaz, Negin Kazemipeourleilabadi, Selin Berk, and İbrahim Kahraman. Their camaraderie have brought immense joy to my Master's experience. The precious times we shared will always hold a special place in my heart.

Last but certainly not least, my biggest thanks go to my family. To my father, Ruhi Tatar, whose constant support has always been a source of strength and encouragement. To my mother Fatma Tatar, whose empathy and compassion have been my refuge. And to my brother Deniz Tatar, who has been more than just a sibling but a best friend and a caring big brother, always there for me.

ABSTRACT

HANDSHAKE PROTOCOLS FOR ENERGY HARVESTING COMMUNICATIONS

This thesis addresses the uncertainty of energy levels in energy-harvesting (EH) wireless communication nodes. Given that EH is inherently random, the energy state of nodes remains unknown, creating challenges in determining optimal transmission times. This uncertainty can lead to inefficient energy usage, as transmissions might occur when the receiver lacks sufficient energy. Therefore, we propose handshake protocols to tackle this energy outage. To address this, we explore the stochastic nature of EH under a Poisson process framework. We analyze the probability mass function (PMF) of battery level for three communication protocols: blind communication with and without acknowledgment, and energy state information (ESI) communication. We also propose mathematical derivations for how long the transmitter node should wait for the receiver node to harvest energy. Through Monte Carlo simulations, we assess the performance metrics of success rate, average delay, and average outage resolution time of these protocols under different battery capacities. Our findings reveal while acknowledgments are sometimes superfluous, sharing energy states significantly enhances energy efficiency and reduces delays between packet receptions. Our study receiver's energy consumption is solely from receiving packets from a single transmitter. In wireless networks, where the nodes sense, transmit, and receive, the PMF of the node's energy level changes significantly. Also this research is built on the assumption energy harvesting follows a Poisson process. Adapting our findings to such network configurations and relaxing our assumptions requires further exploration.

ÖZET

ENERJİ HASADI İLETİŞİMİ İÇİN EL SIKIŞMA PROTOKOLLERİ

Bu tez, enerji hasat eden kablosuz iletişim düğümlerindeki enerji seviyelerinin belirsizliğini ele almaktadır. Enerji hasadının doğası gereği rastgele olduğundan düğümlerin enerji durumu bilinmemekte, bu da optimal iletim zamanlarının belirlenmesinde zorluk yaratmaktadır. Bu belirsizlik, alıcının yeterli enerjiye sahip olmadığı durumlarda gerçekleşen iletimlerin yarıda kesilmesi sonucu verimsiz enerji kullanımına yol açar. İletim anlarındaki enerji kesintisi problemi için bu iki düğüm arasında haberleşmeyi başlatacak el sıkışma protokolleri önerildi. Bunun için enerji hasadının stokastik özellikleri Poisson süreci çerçevesinde incelendi. Üç iletişim protokolü için batarya seviyelerinin olasılık kütle fonksiyonlarını çıkarıldı: onaylamalı ve olmadan kör iletişim ve enerji durumu bilgisi iletişimi. Bu protokollerdeki farklı durumlar için alıcının ne kadar süre enerji hasat etmesi gerektiğine dair bir yöntem önerdik. Monte Carlo simülasyonlarıyla protokollerin performanslarını başarı oranı, ortalama gecikme ve enerji kesitisini ortalama çözme süresi metrikleri üzerinden değerlendirdik. Bulgularımız, onaylamaların bazen gereksiz olduğunu, ancak enerji durumlarının paylaşılmasının enerji verimliliğini artırdığını ve paket alımları arasındaki gecikmeleri azalttığını göstermektedir. Çalışmamızda alıcının enerji tüketimi tek vericiden paket almakla sınırlıdır. Kablosuz ağlarda, alıcının algılama, iletim ve alım gibi görevleri olduğundan, enerji seviyesinin olasılık kütle fonksiyonu değişecektir. Ayrıca, bu araştırmada enerji hasadının Poisson Sürecini takip ettiği varsayılmıştır. Bulgularımızı ağ yapılandırmalarına uyarlamak ve varsayımlarımızı gevşetmek amacıyla yeni çalışmalar yapılabilir.

TABLE OF CONTENTS

LIST OF FIGURES

LIST OF TABLES

LIST OF SYMBOLS

A_i	Energy packets inter-arrival time
C	Total cost of receiving a packet ESI communication
C_k	Energy cost of communication after k'th harvesting period
$C_{R_{pckt}}$	Packet reception energy cost
$C_{T_{ACK}}$	ACK transmission energy cost
$C_{T_{ESI}}$	ESI transmission energy cost
E_k	Battery level after k'th harvesting period
F_{U_τ}	Cumulative density/mass function of energy harvested for τ duration
F_X	Cumulative density/mass function of energy packets
F_X^n	Cumulative density/mass function of sum of n energy packets
f_{E_k}	Probability density/mass function of E_k
f_{R_k}	Probability density/mass function of R_k
f_{U_τ}	Probability density/mass function of energy harvesting for τ duration
f_X	Probability density/mass function of energy packets
f_X^n	Probability density/mass function of sum of n energy packets
k	Order of harvesting periods
l	Packet length
$N_A(t)$	Energy packet arrival process
n	Number of energy packet arrivals
R_k	Residual energy after k'th harvesting period
s	Second
T	Packet generation period
t	Time
t_{out}	Waiting time after an energy outage occur
t_{wait}	Waiting time after an ESI received
U_T	Energy harvesting process for T duration

$U(t)$	Energy harvesting process
u	Energy amount
$X_i(t)$	Size of the i'th energy packet
x	Size of the energy packet
β	Battery capacity
δ	Dirac delta function
λ	Energy packet arrival rate
τ	Energy harvesting duration

LIST OF ACRONYMS/ABBREVIATIONS

ACK	Acknowledgment
AP	Access Point
CDF	Cumulative Distribution Function
CMF	Cumulative Mass Function
EH	Energy Harvesting
ESI	Energy State Information
PDF	Probability Distribution Function
PMF	Probability Mass Function
RF	Radio Frequency
WSN	Wireless Sensor Networks
WuC	Wake-up Call
WuR	Wake-up Radio
WuRTx	Wake-up Radio Transmitter
WuRx	Wake-up Radio Receiver

1. INTRODUCTION

The growing popularity of Internet of things applications and markets has led many researchers to focus on green communication systems with energy harvesting [1]. Energy harvesting is not only for environmental use but also powers the systems without the need for a cable line or constant battery replacement. While the opportunities that EH offers seem promising, EH systems require intelligent and efficient energy policies [2] due to the shortage of energy and the randomness of energy arrivals.

Instantaneous EH power cannot be determined by an observer because harvested energy statistics depend on physical factors such as ambient temperature (thermal energy harvesting), weather conditions (solar or wind energy harvesting), and channel conditions (radio frequency (RF) harvesting) therefore unpredictable [3]. Alternatively, the harvester cannot provide information about the harvested power at all times because it needs to transmit its energy levels wireless or via wired connections. Wireless communication consumes excessive energy, and wired communication conflicts with the nature of EH systems. To ensure that communication protocols work properly in a real-world system, it needs a stochastic understanding of harvested energy with the minimum data from the node, given the energy scarcity in the system (memory, transmission, and processing power consumption costs).

1.1. Motivation and Goal

In a wireless network, two nodes may rely on energy harvesting to sustain their operation and communication. However, due to the uncertainties associated with energy harvesting statics and their own energy consumption, these nodes may not be sure if the other node has sufficient energy to receive their packet. A primary concern is such systems is to establish the initiation of wireless communication effectively.

To address this concern, we have developed a protocol where the transmitter initiates communication by inquiring about the receiver's available energy and estimating the time required for the receiver node to harvest sufficient energy. This approach aims to minimize the energy consumption at the handshaking part and delays due to energy outages during reception. This challenge can be likened to deciding the best time to call a friend who is asleep. If we call every 5 minutes, we disrupt their sleep, preventing rest. On the other hand, waiting 10 hours to call might be too late for conveying important information. We are trying to choose the best time so that our friend gets rest and listen to us.

To resolve this issue, we calculate energy harvesting statistics over time. By acquiring stochastic knowledge of energy arrivals, a node can make an educated estimation of when the receiver node will be ready to engage in communication. This estimation proves to be highly beneficial as it allows nodes to conserve energy by reducing unnecessary transmissions or excessive waiting periods.

Building on this foundational understanding of our energy-aware communication protocol, it becomes evident how it can be seamlessly integrated into various practical energy-harvesting wireless communication applications. In the following sections, specific scenarios illustrate how the protocol adapts to each application, thereby demonstrating its versatility and effectiveness.

1.1.1. Agricultural Networks

For wireless monitoring an orchard or a field multiple sensors are dispersed, alongside access points (AP) [4, 5]. Both the sensors and the AP's might equipped with energy-harvesting mechanisms, with the AP featuring a more powerful energy harvester compared to the sensors. These sensors might be optical, humidity, dielectric soil moisture, electrochemical, and airflow sensors. An example of a such wireless sensor network (WSN) is shown in Figure 1.1

Upon request from the command center, the AP gathers readings for a specific hive by requesting data from the corresponding sensors. Once the data are received, the AP forwards it to the command center. Also command center might send software update data to AP or calibration data to sensors. Also, in this network, additional devices such as irrigation, fertilization, and spraying units can be integrated. The command center might instruct the AP regarding which device to be activated, or deactivated.

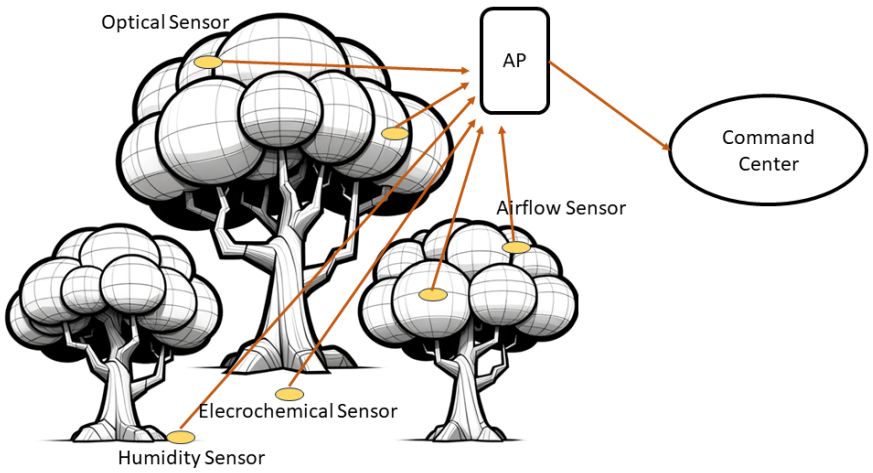

Figure 1.1. Example of an agriculture WSN.

1.1.2. Beehive Networks

Implementing WSN to beehives proves beneficial for the health of the bees and honey production. In these networks [6, 7] sensors are distributed across each hive, and multiple hives are connected to an AP. The types of sensors include sound, temperature, humidity, and motion sensors which monitor vital parameters for the hive. The communication dynamics among sensors, the AP, and the command center mirror those of an agricultural network and it is illustrated in Figure 1.2. In a scenario, both the sensors and the AP are equipped with energy-harvesting structures [6], with the AP boasting a more potent energy harvester than the sensors. There might be two potential scenarios for energy outages exist. Firstly, the AP may face challenges in receiving data from the command center or transmitting data to the command center. Secondly, sensors might lack the energy required to communicate with the AP.

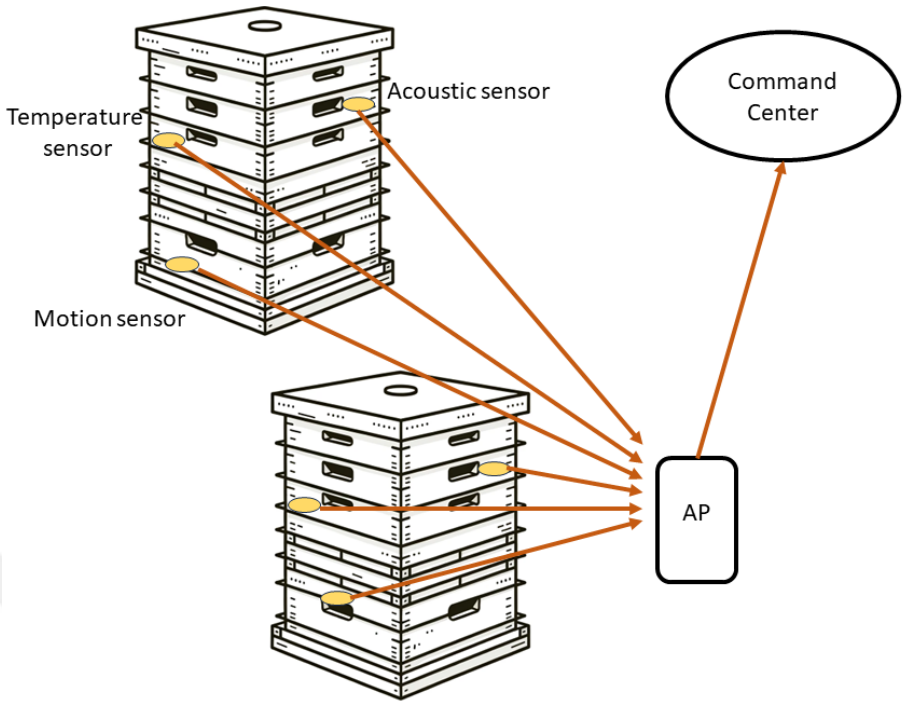

Figure 1.2. Example of a beehive WSN.

1.1.3. Body Area Networks

Energy Harvesting Body Area Networks, as referenced in [8,9], comprise wearable and implanted sensors that track various health metrics, including heart rate, temperature, oxygen saturation, respiration rate, inertial measurements, blood pressure, and electrocardiogram readings. These sensors wirelessly relay collected data to an Access Point (AP), which then forwards the information to a command center, as illustrated in Figure 1.3. While the AP, which may also be an energy-harvesting unit, typically operates under energy constraints, it plays a crucial role in data communication. On receiving a request from the command center, the AP solicits data from the sensors, which, depending on their energy levels, either transmit immediately or wait for a recalculated time to resend their data.

1.2. Energy Efficient WSN Protocols/ Techniques

In this section, we will explain the existing protocols and techniques for energy-efficient networks and how our proposed protocol works along with them.

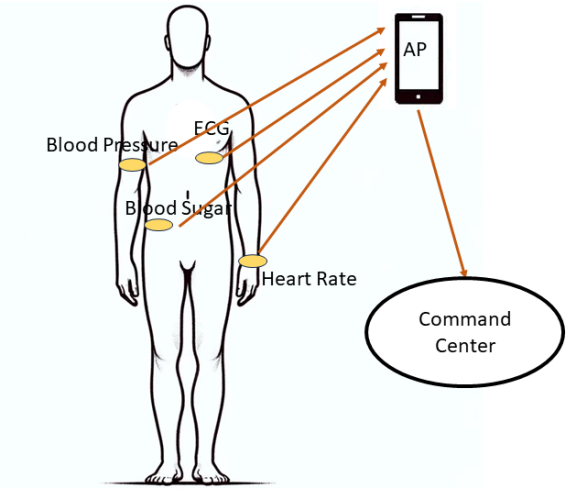

Figure 1.3. Example of a body area WSN.

- Duty cycling and adaptive sleeping involve dynamically adjusting the active and sleep periods of sensor nodes based on their energy harvesting rates and data transmission requirements. By minimizing active time, these strategies effectively reduce energy consumption, thereby extending the network's longevity. In [10], the authors introduce the dynamic sleep scheduling protocol, a centralized method to enhance the lifespan of densely deployed WSN. In [11], the authors introduce the energy-efficient and quality of service aware media access control protocol, which adapts the node's duty cycle based on queue size and packet priority, aiming to minimize delay for high-priority packets and ensure timely delivery. In [12], the authors present a method for achieving energy-neutral operation in EH wireless sensor nodes, employing adaptive duty cycling that aligns with the variable environmental energy availability and the node's instantaneous energy state, allowing the node to sleep during low energy periods and wake when energy is high. Our proposed protocol falls within the adaptive sleeping category. The unique aspect of our approach is that we shift the responsibility for determining the sleeping (harvesting) duration of the receiver to the transmitter, and we also aim to minimize packet delay caused by energy outages in packet receptions. The study in [12] is a good example of the main difference between our work from other methods. In their and much other work such as [13], nodes wake and sense, transmit, etc. depending on their decision but we want to carry this decision to another node who wants to transmit data or request data from the sleeping node.

- Energy-aware routing protocols select routes for data transmission based on the energy levels of the nodes. They avoid nodes with low energy, thus balancing the energy consumption across the network and enhancing its lifespan. In [14], the authors explore a realistic clustering-based WSN model with sensor nodes having random initial energies and varied data generation rates, suitable for heterogeneous sensing applications. It introduces an energy model for this scenario and proposes a traffic and energy aware routing scheme aimed at enhancing the network's stability period. In [15], the authors focus on designing an energy-harvesting-aware routing protocol for heterogeneous Internet of things networks that leverage ambient energy sources. They introduce the energy harvesting aware routing algorithm, which is further augmented by incorporating a novel "energy back-off" parameter to optimize routing efficiency. In their work nodes exchange their energy states as well however in this study they do not consider the energy cost of sharing energy states among the network and the effect of the precision of the shared energy state on the calculations. In addition to that, in our case, we want a node to eventually communicate with a specific node, unlike in a routing problem.
- Data compression techniques reduce the amount of data that needs to be sent, thereby saving energy and increasing throughput. In [16], the authors tackles the challenge of formulating efficient policies for managing lossy data compression tasks for wireless transmission over fading channels, in scenarios characterized by stochastic energy inputs. Additionally in [17], the authors address the limited battery life in small, lightweight wearable devices by employing data compression and wireless transmission speed control. This approach aims to minimize energy consumption for data transmission in these devices, adhering to a deadline constraint. Data compression techniques in our energy-scarce, processing power-lacking system are a luxury for the nodes however in a different environment data compression can work along with our proposed protocol.
- Energy prediction algorithms predict future energy availability based on historical energy harvesting data, allowing for more efficient scheduling of communication and computation tasks. In [18], the authors present an efficient algorithm for

solar energy prediction that considers both seasonal and daily trends, as well as the Sun's diurnal cycle.

- Power management techniques include adaptive transmission power control, where nodes adjust their transmission power based on the distance to the receiving node and the quality of the communication channel. In [19], the authors propose a power management strategy for energy harvesting sensor nodes, focusing on duty-cycle optimization and transmission power control to maximize packet transmission within the limits of variable available energy. In [20], the authors address RF identification communication with energy harvesting tags, evaluating the effects on backscatter modulation and proposing a heuristic transmit power optimization algorithm for active tags in varying channel conditions. Transmitter circuitry is generally the most energy-hungry unit in the wireless nodes therefore avoiding unnecessarily high transmission powers or transmitting with a very low energy so that the receiver cannot decode are both energy waste. In future work of our protocol, channel state information could be passed along with the ESI to avoid such energy wastage.
- Low-power communication technologies like LoRa, Zigbee, or BLE can significantly reduce energy consumption.
- Wake-up radio (WuR) is a low-power radio receiver that remains active while the main radio of a wireless device is in sleep mode. The WuR listens for a specific wake-up signal. When it detects this signal, it activates the main radio, allowing the device to fully wake up and perform regular communication tasks. This approach significantly reduces power consumption since the WuR consumes much less energy compared to the main radio being active all the time. The article [21] explores the advantages and challenges of wake-up receivers, providing an overview of cutting-edge hardware and protocol proposals, and discussing new potential application areas for these receivers.

1.3. Energy Harvesting Methods and Models

There are many types of energy-harvesting processes employed in WSNs, such as solar energy harvesting, kinetic energy harvesting, RF energy harvesting, and thermoelectric harvesting. Each of these methods is distinct in how they capture and convert energy:

- Solar energy harvesting involves using photovoltaic cells to convert sunlight into electrical energy. It is particularly effective in outdoor environments [9] with ample sunlight but can be less reliable in cloudy or indoor conditions.
- Kinetic energy harvesting captures energy from motion or mechanical vibrations. It is useful in environments where motion is constant or frequent, such as on machinery or human-worn devices. In [22], the authors concentrate on characterizing the kinetic energy harvested by wireless nodes and developing energy allocation algorithms for them, describing methods to estimate energy from acceleration traces and characterizing energy availability associated with human activities like relaxing, walking, and cycling.
- RF energy harvesting capturing energy from ambient or dedicated RF sources. It is beneficial in environments where RF signals are strong and consistent, like near communication networks or in urban areas. In [23], the authors propose a new medium access control protocol aimed at enhancing energy efficiency in wireless local area networks. Their protocol facilitates selective RF energy transfer requests based on a device's residual energy.
- Thermoelectric harvesting converts temperature differences into electrical energy. It is effective in environments with varying temperatures or where heat is a byproduct of processes. In [24], the authors report on a thermoelectric energy harvesting system for nuclear plants, capable of operating in high radiation and utilizing waste heat to power wireless sensors for enhanced safety, functioning in both standard and emergency conditions

1.4. Energy Consumption of Wireless Sensor Nodes

In a wireless sensor, energy consumption is typically divided into several key blocks or components. The list of the primary energy consumption blocks in a wireless sensor:

- Communication unit manages wireless communication, sending and receiving data. It usually consumes the most energy, especially during data transmission over wireless channels. Includes components like a transmitter, receiver, and sometimes a separate module for signal modulation and demodulation.
- Microcontroller unit processes the data collected by the sensing unit. It includes tasks like data filtering, aggregation, and compression. The energy consumption here depends on the complexity of the processing tasks and the efficiency of the microcontroller.
- WuR in WSN serves as a low-power alternative to traditional radio transceivers, primarily aimed at reducing the energy consumption associated with the main transceiver's idle listening. Although WuR offers significantly greater energy efficiency compared to the main transceiver, it still incurs energy usage during idle listening, as well as during the transmission, and reception of wake-up signals.
- The power management unit is a crucial component of the sensor, tasked with efficiently managing and distributing power. It encompasses voltage regulation and power conversion (such as DC-DC converters). Its main energy consumption is attributed to energy leakages, non-ideal power conversion, and non-ideal power transfer among the units.
- Memory (storage) unit used for storing data and program instructions. Includes both volatile (RAM) and non-volatile memory (flash storage). Energy is used during data read, write, and erase operations.
- Idle and sleep modes are the least energy consuming modes of the node, however. energy is still consumed. Includes keeping minimal circuitry operational for quick wake-up and maintaining state information.
- Sensing block is responsible for capturing physical or environmental data like

temperature, humidity, light, motion, etc. Energy is used to power the sensors and convert the physical parameters into electrical signals.

1.4.1. Outline

The rest of the thesis is organized as follows. In Chapter 2, we delve into the derivation of stochastic formulas for the energy harvesting process, focusing on Poisson energy packet arrivals. Chapter 3 presents an in-depth explanation of the system model, including the study of the protocols: blind communication without ACK, blind communication with ACK, and ESI communication. This chapter also covers the energy consumption implications of these protocols. Moving to Chapter 4, the analysis shifts to the battery energy levels of the three protocols. Chapter 5 presents the results of our studies, offering a comprehensive discussion of the findings from the previous chapters, including simulations and data analysis. Finally, Chapter 6 concludes the thesis by summarizing the key results and discussing potential avenues for future work on the ESI.

2. ENERGY HARVESTING MODEL

Exploring energy management in WSN, our study emphasizes understanding the dynamics of energy harvesting. We adopt a systematic approach to analyzing energy packet arrivals, focusing on their patterns and impacts. This inquiry is vital for grasping the operational efficiency of these networks. In our model, we conceptualize energy harvesting as a process where energy packets arrive following a Poisson distribution, as supported by [25], [26], and [27]. We define A_i as the inter-arrival time, which is the time interval between i'th and $(i-1)$'st energy packet. Additionally, X_i denotes the size of the i'th energy packet. Therefore we can express the harvested energy from 0 to time t as

$$U(t) = \sum_{i=1}^{N_A(t)} X_i, \tag{2.1}$$

where $N_A(t) = \max(k : A_1 + A_2 + \cdots + A_k \leq t)$ indicates the number of energy packet arrivals up to time t. Thus, $U(t)$ is a cumulative stochastic process. A_i and X_i are assumed to be independent of each other, and X_i's are assumed to be independent and identically distributed (i.i.d) random variables. The energy packet arrival process is shown in Figure 2.1. The harvested energy amount for any given starting point t can be expressed as

$$\begin{aligned} P(U(t+\tau) - U(t) = u) &= P\left(\sum_{i=1}^{N_A(t+\tau)} X_i - \sum_{i=1}^{N_A(t)} X_i = u\right) \\ &= P\left(\sum_{i=N_A(t)+1}^{N_A(t+\tau)} X_i = u\right). \end{aligned} \tag{2.2}$$

Due to the memoryless property of the Poisson process, the number of energy packet arrivals in the interval of $(t, t+\tau]$, which is denoted as $N_A(t+\tau) - N_A(t)$, also follows a Poisson distribution. Consequently, the probability $P(N_A(t+\tau) - N_A(t) = n)$ is equivalent to $P(N_A(\tau) = n)$. Because X_i values are i.i.d, Equation (2.2) can be simplified to

$$\begin{aligned} P(U(t+\tau)-U(t)=u) &= P\left(\sum_{i=1}^{N_A(t+\tau)-N_A(t)} X_i = u\right) \\ &= P\left(\sum_{i=1}^{N_A(\tau)} X_i = u\right) \\ &= P(U(\tau)=u). \end{aligned} \tag{2.3}$$

This indicates that the energy harvesting process $U(\tau)$ over a specified duration τ is independent of the starting point t, thus the process is stationary. For the sake of simplicity, we will represent the harvested energy for any starting point t, over a duration of τ time, as

$$U_\tau = U(t+\tau) - U(t). \tag{2.4}$$

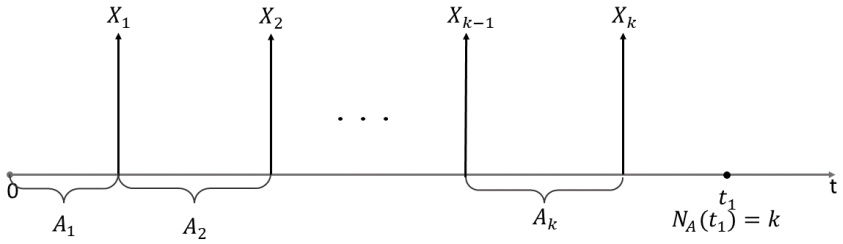

Figure 2.1. Energy packet arrivals.

To determine the probability of harvesting u units of energy over a duration of τ we need to calculate the probabilities associated with both the number of packets arriving and the total energy carried by these packets. The probability of the number of packets arriving within τ time can be obtained using the PMF of the Poisson distribution which is expressed as

$$P(N_A(\tau)=n) = e^{-\lambda\tau}\frac{(\lambda\tau)^n}{n!}, \qquad n=0,1,\ldots. \tag{2.5}$$

The probability density function (PDF) of the total energy carried by these n packets can be found as the recursive function shown as

$$f_X^{(n)} = f_X^{(n-1)} * f_X, \qquad n=0,1, \tag{2.6}$$

where f_X is the PDF of the energy packet sizes, $*$ is the convolution operator and the $f_X^{(n)}$ is the PDF of the total energy of the n energy packets. The cumulative distribution function (CDF) of the total energy of the n energy packets can be recursively determined as

$$\begin{aligned} F_X^{(n)}(u) &= \int_{-\infty}^{u} f_X^{(n)}(x)dx \\ &= \int_{-\infty}^{u}\int_{-\infty}^{\infty} f_X^{(n-1)}(w-x)f_X(x)dwdx \\ &= \int_{-\infty}^{\infty}\int_{-\infty}^{u} f_X^{(n-1)}(w-x)dwf_X(x)dx \\ &= \int_{-\infty}^{\infty} F_X^{(n-1)}(u-x)dF_X(x). \end{aligned} \tag{2.7}$$

Then the probability that the total energy of the incoming n packets is less than u units energy expressed as

$$P(U_\tau \leq u, N_A(t) = n) = e^{-\lambda\tau}\frac{(\lambda\tau)^n}{n!}F_X^{(n)}(u). \tag{2.8}$$

Finally, to find the CDF of the U_τ, a summation over all possible numbers of packets is performed as

$$P(U_\tau \leq u) = F_{U_\tau}(u) = \sum_{n=0}^{\infty} e^{-\lambda\tau}\frac{(\lambda\tau)^n}{n!}F_X^{(n)}(u). \tag{2.9}$$

PDF of the U_τ is found as

$$\begin{aligned} \frac{d(F_{U_\tau}(u))}{du} &= \frac{d\left(\sum_{n=0}^{\infty} e^{-\lambda\tau}\frac{(\lambda\tau)^n}{n!}(F_X^{(n)}(u))\right)}{du} \\ f_{U_\tau}(u) &= \sum_{n=0}^{\infty} e^{-\lambda\tau}\frac{(\lambda\tau)^n}{n!}f_X^{(n)}(u). \end{aligned} \tag{2.10}$$

2.1. Discrete Random Energy Packet Sizes

If we assume X_i is a discrete random variable, then f_X in Equation (2.10) becomes the PMF of the energy packet sizes. Similarly, $f_X^{(n)}$ is the PMF of the sum of n energy packets. Therefore, the probability of harvesting total energy of u over τ is equivalent to the expression given in Equation (2.10).

2.2. Deterministic Energy Packet Sizes

If we assume energy packet sizes X_i is deterministic and equal to x, randomness is solely from the number of arrivals therefore Equation (2.10) changes to

$$P(U_\tau = u) = \begin{cases} e^{-\lambda\tau} \dfrac{(\lambda\tau)^{\frac{u}{x}}}{\left(\frac{u}{x}\right)!} & \text{if } u/x \text{ integer} \\ 0 & \text{else.} \end{cases} \tag{2.11}$$

Therefore cumulative mass function (CMF) can be expressed as

$$P(U_\tau \leq u) = \sum_{n=0}^{\left\lfloor \frac{u}{x} \right\rfloor} e^{-\lambda\tau} \frac{(\lambda\tau)^n}{n!}. \tag{2.12}$$

3. SYSTEM MODEL

In our research, we explore three distinct communication protocols, which we have designated as blind communication without ACK, blind communication with ACK, and ESI communication. The names of the first two protocols are self-explanatory. The first protocol transmits the data packet without concern for whether it is received or not. The second protocol transmits its data packets and waits for an ACK. If it does not receive one, it retransmits the data packet. In the third protocol, the transmitter first inquires about the receiver's ESI and sends its data if the receiver has enough energy.

We investigated the protocols under a noiseless environment; therefore, the only reason for a packet, an ESI, or an ACK to be lost is due to an energy outage event. Additionally, since energy harvesting power is very scarce, the harvesting durations are relatively longer than the communication duration. Therefore, we assume that transmissions and receptions occur instantaneously and that harvesting is never interrupted. Which also indicates that we ignore propagation, processing, transmission delays.

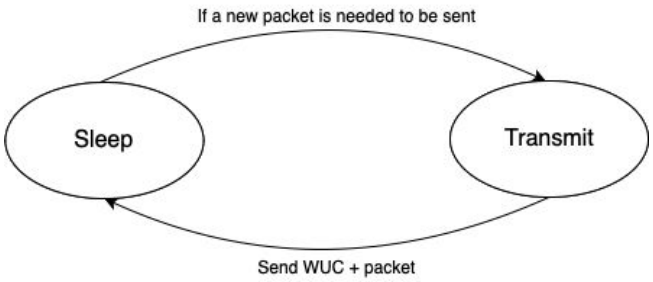

Figure 3.1. State diagram depicting the protocol for the blind communication without ACK.

The communication state diagrams of the protocols are illustrated in Figures 3.1, 3.2, and 3.3 offering a detailed visual representation. Each diagram shows the operational states of the transmitter node and cases for the state transitions for the corresponding protocol.

The first diagram is shown in Figure 3.1, we see the state diagram of the blind communication without ACK and there are two states. The transmitter node starts in the sleep state, where it waits for a data packet to be generated. Every T time, a data packet is generated to be transmitted. When the data packet generated after T time, the transmitter transitions to the transmit state and sends a wake-up call (WuC). Normally receiver node is in the sleep state with its main receiver circuitry off to save energy. Therefore transmitter needs to wake the receiver by sending WuC call and start a wake up handshake. After the wake up handshake completes the transmitter sends the data packet. Afterward, it returns to the sleep state and remains there for T time.

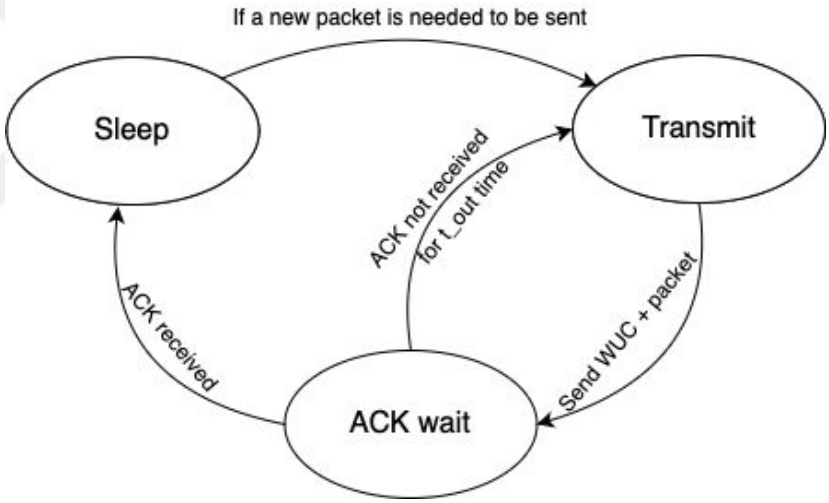

Figure 3.2. State diagram depicting the protocol for the blind communication with ACK.

In the second diagram, Figure 3.2, there are three states for the blind communication with ACK. The node starts in the sleep state and waits T time until a data packet is generated to be sent. It then moves to the transmit state, sends a WuC and the data packet, and subsequently enters the ACK waiting state. Upon the receiver's reception of the data packet, the receiver sends an ACK, and the transmitter returns to the sleep state. However, if no ACK is received by the transmitter within a certain timeout period t_{out}, the transmitter reverts to the transmit state and retransmits the data packet.

In the third and final diagram, Figure 3.3, there are six states. When a data packet is ready to be sent, the transmitter enters the send WuC state. After transmitting the WuC, it moves to the ESI waiting state. If no ESI packet is received within the t_{out} time, the transmitter goes back to the send WuC state. Once an ESI packet is received, the transmitter enters the wait state and calculates how long it needs to wait t_{wait} for the receiver to harvest enough energy. Then, it transitions to the transmit state and sends the WuC and the data packet. After the transmission is complete, it enters the ACK wait state. If an ACK is received, it returns to the sleep state; if no ACK is received within the t_{out} time, the transmitter goes back to the send WuC state.

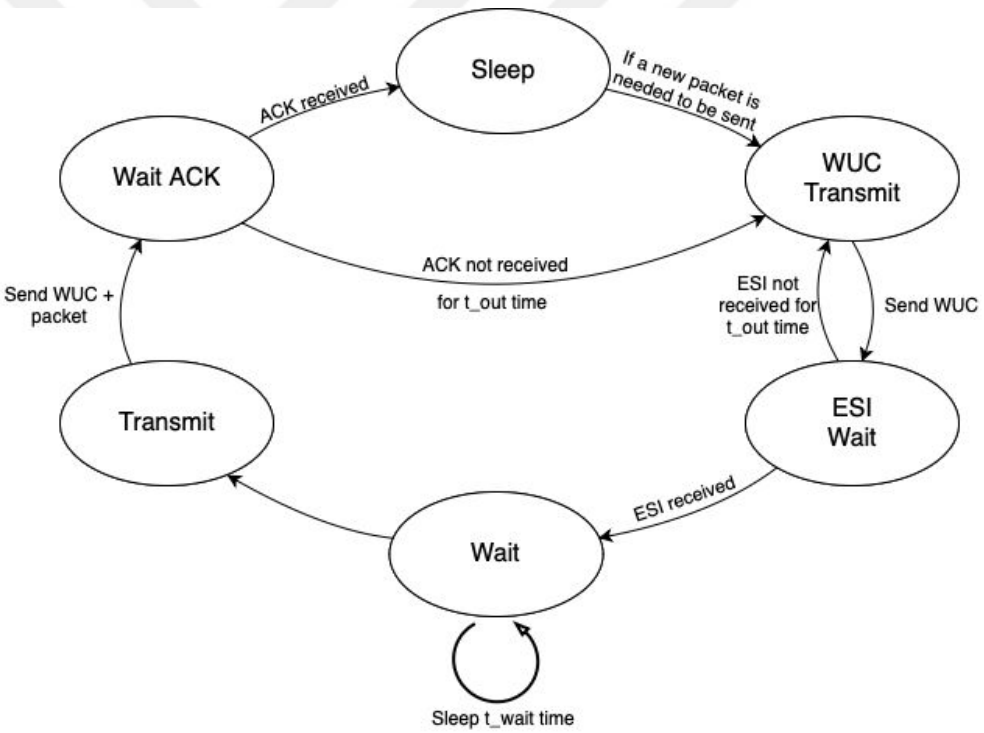

Figure 3.3. State diagram depicting the protocol for the ESI communication protocol.

To fully solidify our system we also need to analyze energy consumption in nodes, researchers focus on the energy consumption per bit and have developed various formulations. These models vary depending on the application and environment, as some are tailored for urban areas while others are for rural settings. The range of operation also influences these models, with some designed for close range (1-10 m) and others for medium range (10-100 m). Additionally, the length of the data packets, whether

long or short, impacts the energy consumption per bit. These aspects are thoroughly explored in surveys and papers. In our model, there are three main sources of energy consumption. Receiving packet energy cost ($C_{R_{pckt}}$), For the receiving unit, our model includes components such as a low-noise amplifier, a frequency mixer, three types of filters, an intermediate frequency amplifier, and an analog-to-digital converter. The schematic of this receiver circuitry is depicted in Figure 3.4. [28] provides an in-depth analysis of the energy consumption characteristics of these components. The energy usage here primarily depends on the packet's duration and the energy required to transition from a sleeping state to active listening. Transmitting ACK for packet $C_{T_{ack}}$, The transmitter consists of a digital-to-analog converter, two filters, a mixer, and a power amplifier. The transmitter circuit block is depicted in Figure 3.4. The cost of transmitting a signal mainly depends on both the distance and duration of the signal. The energy consumption is explained in more detail in [28]. Transmitting ESI energy cost $C_{T_{ESI}}$ The energy cost of transmitting ESI is the same as that of transmitting an ACK. Main circuitry and WuR circuitry sleeping power consumption is negligible.

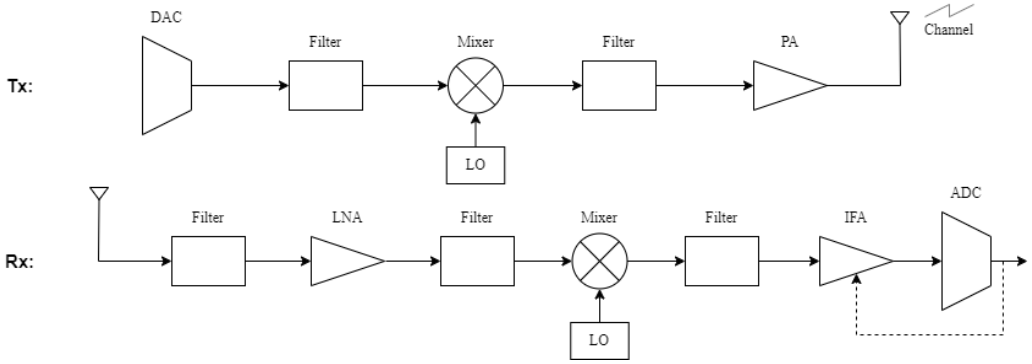

Figure 3.4. Transmitter and receiver circuit blocks.

4. ANALYSIS OF BATTERY ENERGY LEVEL

We have discussed the energy harvesting principles related to the receiver. The battery level of the receiver node is a random process, depending not only on the energy harvesting process but also on the protocol and battery capacity. This is because the protocol dictates how the energy will be consumed, and the battery capacity imposes an energy constraint on the maximum energy stored. In the following sections, we will discuss the process of the battery's energy level in more detail.

4.1. Blind Communication without ACK

In this section, we examine the battery level of the receiver under a specific condition, namely when blind communication without an ACK protocol is employed. The mathematical representation of the battery level can be formulated as

$$E_k = \max(\beta, R_{k-1} + U_\tau), \qquad \tau \in T,\ k \in 1, 2, \ldots, \tag{4.1}$$

where E_k denotes the battery level after the k'th harvesting period, β represents the maximum battery capacity, and R_{k-1} is the residual energy in the battery before the k'th harvesting period. The concept of residual energy, critical in this context, pertains to the energy remaining in the battery after communication activities. This residual energy is defined as

$$R_k = \max(E_k - C_k, 0) \tag{4.2}$$

with C_k signifying the energy expenditure for k'th the communication. Which is expressed as

$$C_k = C_{R_{pckt}}. \tag{4.3}$$

The sub-notation representations provided may not be immediately intuitive at first glance. Hence, for enhanced clarity and better understanding, Figure 4.1, and 4.2 have been included.

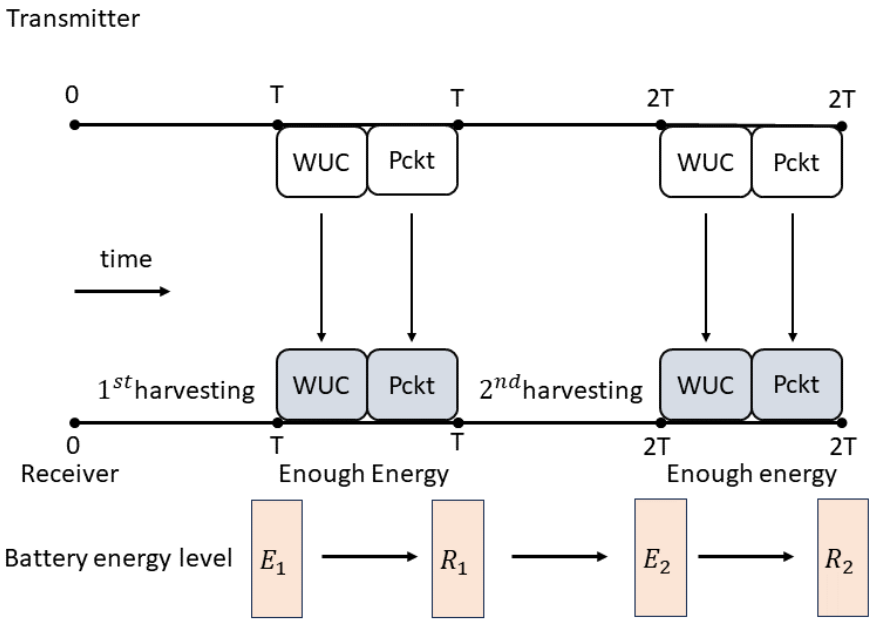

Figure 4.1. Packet transmission and battery energy level when the receiver has enough energy in blind communication without ACK.

4.1.1. Energy Level Prediction

In scenarios where nodes do not exchange ESI and ACK, data transmission and reception occur blindly. Under such circumstances, the transmitter will initiate data transmission without the receiver having adequate energy to successfully receive the packet. This will result in the receiver depleting its battery while attempting to receive the packet because we assume that receiver do not know how much energy needed to receive the packet and after wake up call receiver tries to receive the packet with its last energy in the battery. Consequently, in cases of successful data packet receptions, the residual energy is calculated using Equation (4.2) and the PMF of E_{k+1} can thus be expressed using Equations (4.1), and (4.2) as

$$f_{E_{k+1}} = \begin{cases} f_{R_k} * f_{U_T} & \text{if } E_{k+1} < \beta \\ 1 - F_{E_{k+1}}(\beta - 1) & \text{if } E_{k+1} = \beta \\ 0 & \text{if } E_{k+1} > \beta. \end{cases} \tag{4.4}$$

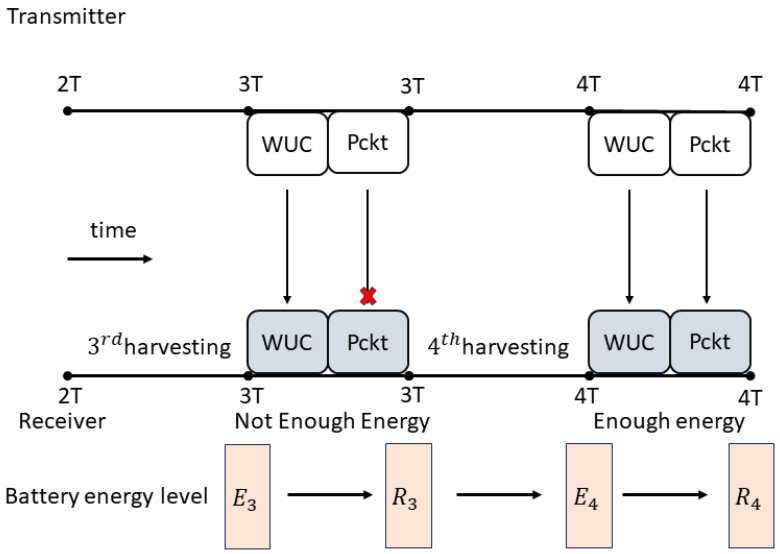

Figure 4.2. Packet transmission and battery energy level when the receiver does not have enough energy in blind communication without ACK.

4.1.1.1. Minimum Battery Capacity. The term minimum battery capacity refers to a scenario where the receiver's battery capacity is just sufficient for the reception of a single data packet. Consequently, when a successful communication occurs, there will be no energy remaining in the battery, denoted as $R_k = 0$. Similarly, in the event of an energy outage, the residual energy in the battery will also be $R_k = 0$. Given these conditions PMF of the E_{k+1} can be expressed as

$$f_{E_{k+1}} = \begin{cases} f_{U_T} & \text{if } E_{k+1} < \beta \\ 1 - F_{E_{k+1}}(\beta - 1) & \text{if } E_{k+1} = \beta \\ 0 & \text{if } E_{k+1} > \beta. \end{cases} \tag{4.5}$$

4.1.1.2. Finite Battery Capacity. In the case of finite battery capacity after the data packet reception, there might be residual energy in the battery. The residual energy affects the PMF of E_{k+1} as explained in Equation (4.4). Additionally, we can find the PMF of R_k using Equation (4.2) as

$$f_{R_k}(r_k) = \begin{cases} \sum_{u=0}^{C_k} f_{E_k}(u) & \text{if } r_k = 0 \\ f_{E_k}(r_k + C_k) & \text{if } r_k \neq 0. \end{cases} \tag{4.6}$$

This shows us knowledge of E_k removes the uncertainty of the R_k. In Figure 4.3 we see the relation between R_k and the E_k.

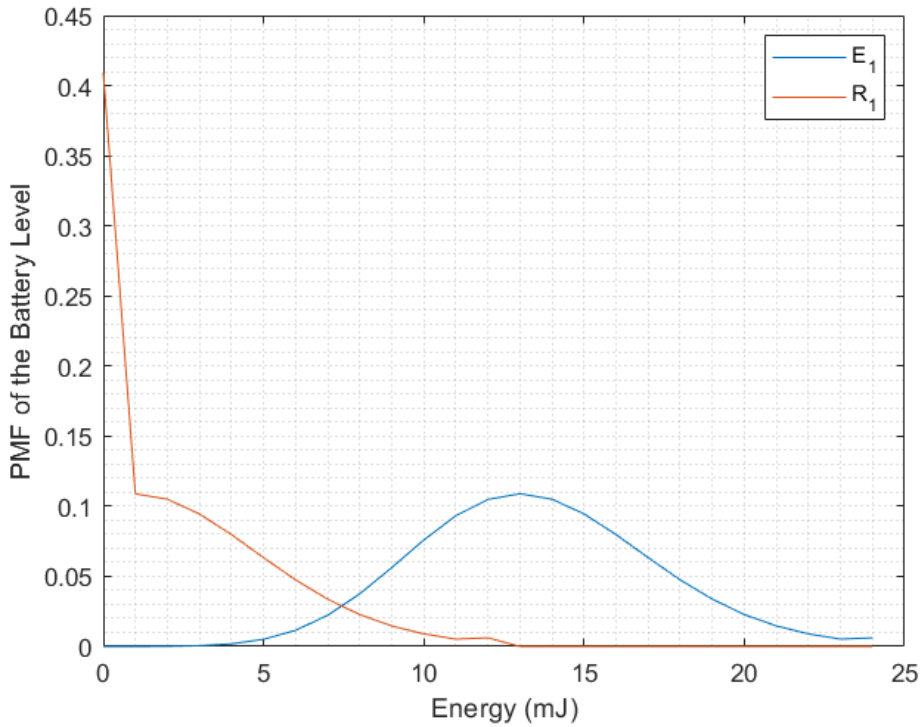

Figure 4.3. The PMF of the E_k and R_k in the blind communication without ACK when $\beta = 24$, $C_k = 12$, $\lambda = 0.15$.

In Equation (4.4) there are 3 cases due to the limited battery capacity however calculating the first case is enough to find the PMF therefore we can expand Equation (4.4) as

$$\begin{aligned} f_{E_{k+1}}(e_{k+1}) &= \sum_{u=0}^{C_k} f_{E_k}(u) \cdot f_{U_T}(e_{k+1}) \\ &+ \sum_{r=1}^{\beta - C_k} f_{E_k}(r + C_k) \cdot f_{U_T}(e_{k+1} - r) \quad 0 \leq e < \beta. \end{aligned} \tag{4.7}$$

This shows that the f_{E_k} is dependent on k so the PMF changes after every harvesting duration. In the Figure 4.4 we see the behaviour of the f_{E_k} as k increases. And it is seen that f_{E_k} converges to a steady state $f_{E_{ss}}$.

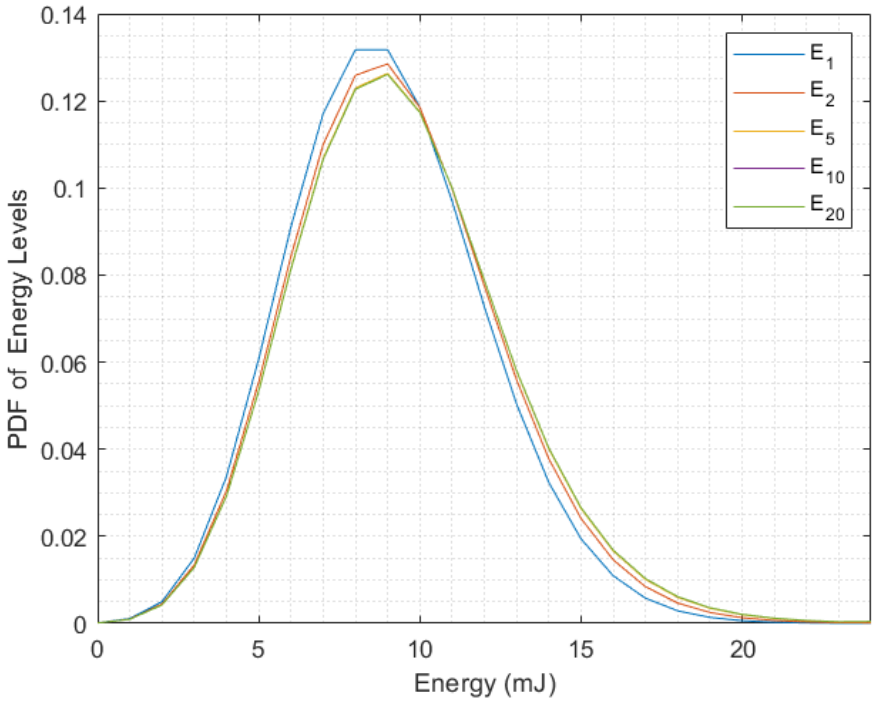

Figure 4.4. The PMF of the E_k's as k increases in the blind communication without ACK when $\beta = 24$ mJ, $C_k = 12$ mJ, $T = 60$ s, $\lambda = 0.15$.

4.1.1.3. Infinite Battery Capacity. In the infinite battery case, we assume that the battery is large enough that it never goes to overcharging. We saw that in our simulations a small coin cell battery with 10.8 J capacity is big enough that it never overcharges. The calculations for infinite battery capacity is similar to the finite battery, only the β battery capacity constraints drop. So Equation (4.4) simplifies to

$$f_{E_{k+1}} = f_{R_k} * f_{U_T} \tag{4.8}$$

because the battery never goes overcharged. And Equation (4.7) simplifies to

$$\begin{aligned} f_{E_{k+1}}(e_{k+1}) &= \sum_{u=0}^{C_k} f_{E_k}(u) \cdot f_{U_T}(e_{k+1}) \\ &+ \sum_{r=1}^{\infty} f_{E_k}(r + C_k) \cdot f_{U_T}(e_{k+1} - r), \quad e_k \geq 0. \end{aligned} \tag{4.9}$$

4.1.2. Calculating the Harvesting Time

The statistics of energy harvesting and residual energy have been discussed in the preceding sections. Now, we are in a position to establish a relationship between the probability of the receiver successfully receiving a packet and the duration of energy harvesting. Let's denote this probability as $P(\text{success})$. In this protocol, the only adjustable parameter for the transmitter is the duration T. Hence, we can define $P(\text{success})$ as

$$\begin{aligned} P(\text{success}) &= P(E_{k+1} \geq C_k) = \sum_{i=0}^{\beta - C_k} P(E_{k+1} \geq C_k | R_k = i) P(R_{k-1} = i) \\ &= \sum_{i=0}^{\beta - C_k} P(R_k + U_T \geq C_k | R_k = i) P(R_k = i) \\ &= \sum_{i=0}^{\beta - C_k} P(U_T \geq C_k - i | R_k = i) P(R_k = i). \end{aligned} \tag{4.10}$$

When the energy remaining in the battery capacity exceeds the C_k, sometimes after packet reception some energy will be left in the battery. This residual energy is then combined with the energy harvested in the next cycle. PMF of this residual energy is dependent to the battery capacity therefore we will investigate it under different battery capacities.

4.1.2.1. Minimum Battery Capacity. When the battery level is equal to C_k, no residual energy remains in the battery following packet receptions, or in scenarios of energy outages. Consequently, under these conditions, Equation (4.10) can be simplified to

$$P(\text{success}) = P(U_T \geq C_k). \tag{4.11}$$

4.1.2.2. Finite Battery Capacity. When the battery level is not the minimum we can use our numerical solution of the $f_{E_{ss}}$ which can be expressed as

$$P(\text{success}) = \sum_{u=C_k}^{\beta} f_{E_{ss}}(u). \tag{4.12}$$

4.1.2.3. Infinite Battery Capacity. In this case, we use Equation (4.12) to calculate the P(success) however the capacity constraint β drops. It is important to know that in the infinite battery case as explained in the [29], outage probability convergence to 0 when harvested energy is equal to the consumed energy in the mean case.

4.2. Blind Communication with ACK

The battery level of the receiver when employing blind communication with an ACK protocol can be shown as

$$E_k = \max(\beta, R_{k-1} + U_\tau), \qquad \tau \in \{T, t_{out}\},\ k \in 1, 2 \ldots. \tag{4.13}$$

The primary distinction from Equation (4.1) lies in the dependency of the harvesting durations on the outcome of the previous communication. Specifically, in instances where reception fails, the transmitter will wait for a duration of t_{out} time instead of T time. The energy level of the receiver's battery throughout successful receptions is shown in Figure 4.5 and an outage event and resolution of the outage with respect to the harvesting periods and the battery levels is shown in Figure 4.6. The residual energy after receiving an ACK is expressed as

$$R_k = \begin{cases} \max(E_k - C_k, -C_{T_{ACK}}) & \text{if success} \\ \max(E_k - C_k, 0) & \text{if outage.} \end{cases} \tag{4.14}$$

It is crucial to note that although we allow R_k to take negative values in our model, in reality, negative energy does not exist. This modeling approach is adopted under the assumption that after receiving data, the receiver has a time window of t_{out} to send an ACK. Therefore, the concept of negative energy, in our assumption represents energy borrowing from the following energy harvesting period. This assumption simplifies the calculations. Therefore we can express C_k as

$$C_k = \begin{cases} C_{R_{pckt}} + C_{T_{ACK}} & \text{if success} \\ C_{R_{pckt}} & \text{if outage.} \end{cases} \tag{4.15}$$

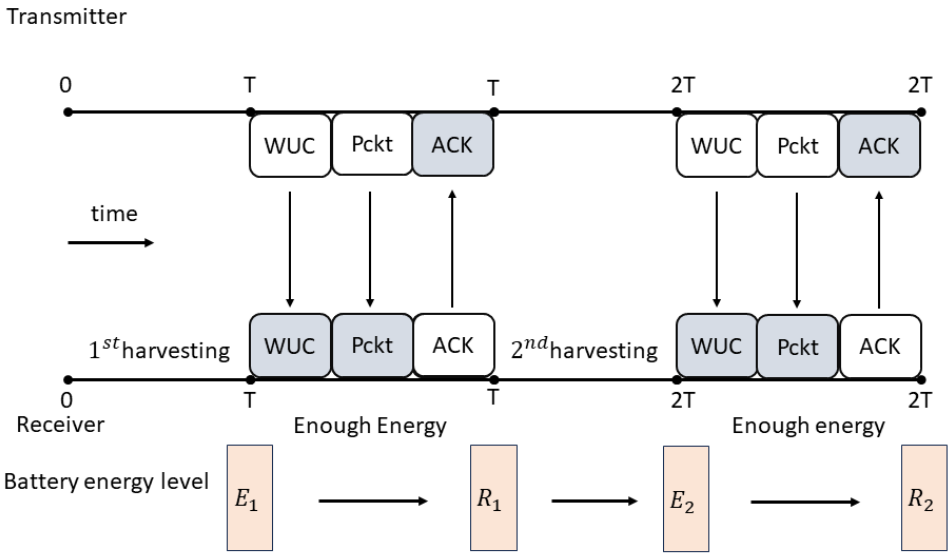

Figure 4.5. Packet transmission and battery energy level when the receiver has enough energy in blind communication with ACK.

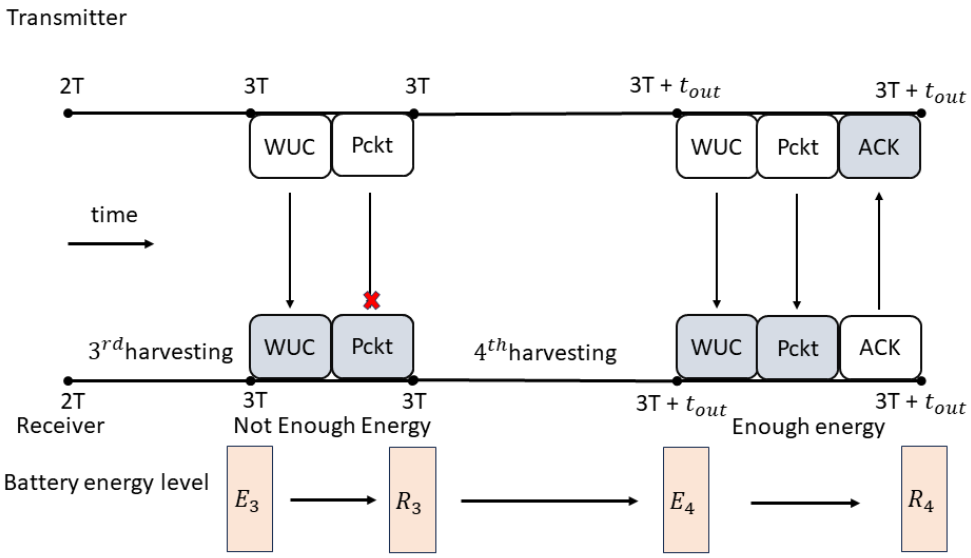

Figure 4.6. Packet transmission and battery energy level when the receiver does not have enough energy in blind communication with ACK.

4.2.1. Energy Level Prediction

There are two outcomes that influence the calculation of the next energy level. In the event of an outage, the transmitter will be aware that $R_k = 0$. Conversely, if the transmitter successfully receives an ACK, the residual energy is determined

using Equation (4.14). Consequently, E_{k+1} for both scenarios can be described using Equations (4.13) and (4.14) as

$$f_{E_{k+1}} = \begin{cases} f_{R_k} * f_{U_T} & \text{if } E_{k+1} < \beta \\ 1 - F_{E_{k+1}}(\beta - 1) & \text{if } E_{k+1} = \beta \\ 0 & \text{if } E_{k+1} > \beta. \end{cases} \tag{4.16}$$

4.2.1.1. Minimum Battery Capacity. When a successful communication takes place, the transmitter will be aware that $R_k = -C_{T_{ACK}}$. In the event of an energy outage, no residual energy will remain in the battery, which is denoted as $R_k = 0$. Therefore, following a successful reception, the PMF of the E_{k+1} can be expressed as

$$f_{E_{k+1}|\text{ACK}} = \begin{cases} \delta(-C_{T_{ACK}}) * f_{U_T} & \text{if } E_{k+1} < \beta \\ 1 - F_{E_{k+1}|ACK}(\beta - 1) & \text{if } E_{k+1} = \beta \\ 0 & \text{if } E_{k+1} > \beta, \end{cases} \tag{4.17}$$

where ACK means acknowledgment received and $\delta(-C_{T_{ACK}})$ represents the Dirac Delta function at $-C_{T_{ACK}}$. Therefore with the convolution operation $f_{E_{k+1}|ACK}$ will be equal to left shifted f_{U_T}. Furthermore, in the event of an energy outage, the PMF of E_{k+1} can be expressed as

$$f_{E_{k+1}|out} = \begin{cases} f_{U_{t_{out}}} & \text{if } E_{k+1} < \beta \\ 1 - F_{E_{k+1}|out}(\beta - 1) & \text{if } E_{k+1} = \beta \\ 0 & \text{if } E_{k+1} > \beta, \end{cases} \tag{4.18}$$

where *out* means an energy outage occurred.

4.2.1.2. Finite Battery Capacity. In the context of a finite battery, the failure to receive an ACK indicates to the transmitter that an energy outage has transpired, hence $R_k = 0$ Accordingly, the next energy level's estimation utilizes Equation (4.18). When an acknowledgment is received, it denotes that the receiver's energy level was greater than or equals to $C_{R_{pckt}}$. Then the receiver expends $C_{R_{pckt}}$ energy to process the in-

coming data packet. Therefore, for situations where an ACK is received, the PMF of R_k can be calculated as

$$f_{R_k|ACK}(r|ACK) = \frac{f_{E_k}(r + C_k)}{1 - F_{E_k}(C_{R_{pckt}})}. \tag{4.19}$$

Then to estimate the next energy level we can insert this PMF into the first case of Equation (4.16) which results as

$$f_{E_{k+1}} = \frac{f_{E_k}(r + C_k)}{1 - F_{E_k}(C_{R_{pckt}})} * f_{U_T}. \tag{4.20}$$

As in blind communication without ACK next energy level is dependent on the previous level however a steady state convergence is also observed in this case which is shown in Figure 4.7.

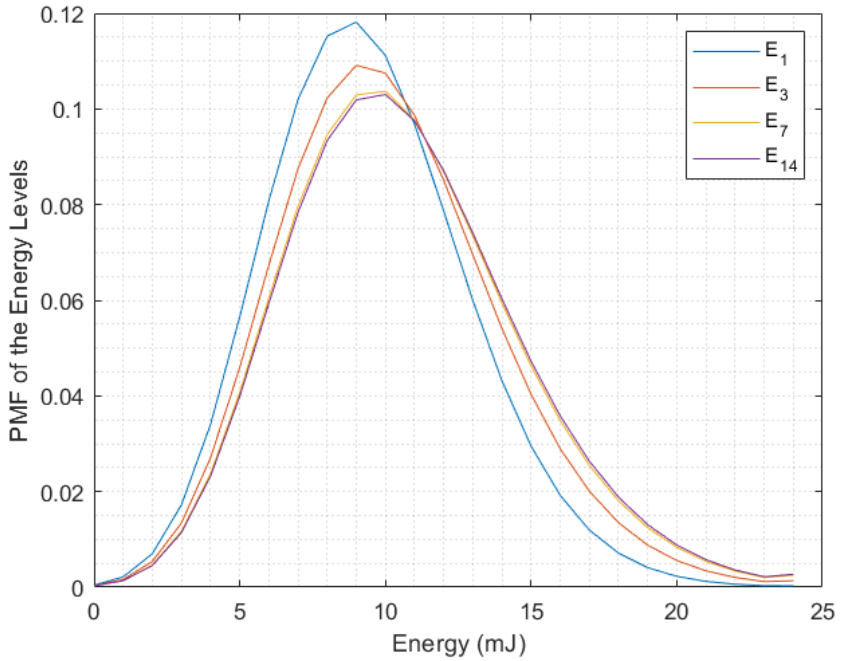

Figure 4.7. A numerical example of the convergent behavior of the PMF of the E_k after successive successful packet receptions in blind communication with ACK when $\beta = 24$ mJ, $C_{R_{pckt}} = 12$ mJ, $C_{T_{ACK}} = 1$ mJ, $\lambda = 0.15$.

4.2.1.3. Infinite Battery Capacity. The infinite battery case is the same as the finite battery case just without the battery capacity constraint. We use Equation (4.18) to estimate the next energy level after an outage and we use Equation (4.20) after an ACK reception. The convergent behavior of the f_{E_k} after successive successful receptions is

shown in Figure 4.8. It is important to highlight that convergence only occurs after successive receptions. Whenever an outage occurs the PMF of the E_k goes back to the E_1 shown in Figure 4.8.

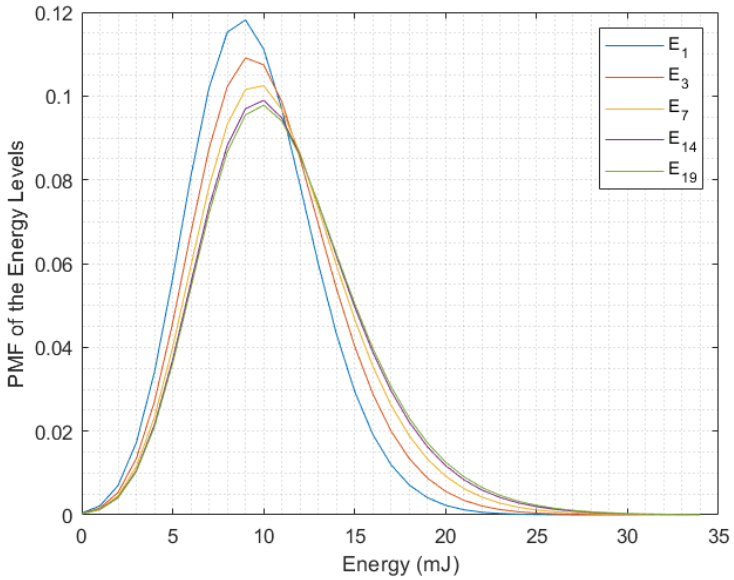

Figure 4.8. A numerical example of the convergent behavior of the PMF of the E_k after successive successful packet receptions in blind communication with ACK when $\beta = \infty$, $C_{R_{pckt}} = 12$ mJ, $C_{T_{ACK}} = 1$ mJ, $\lambda = 0.15$.

4.2.2. Calculating the Harvesting Time

In this protocol, we need to derive the success probability under two scenarios which depend on the reception of the ACK, namely after a successful reception and after an energy outage. We begin by deriving the P(success after transmission) using Equation (4.16) which is expressed as

$$\begin{aligned} P(\text{success after transmission}) &= P(E_{k+1} \geq C_k) \\ &= \sum_{i=-C_{T_{ACK}}}^{\beta - C_k} P(E_{k+1} \geq C_k | R_k = i) P(R_k = i) \\ &= \sum_{i=-C_{T_{ACK}}}^{\beta - C_k} P(R_k + U_T \geq C_k | R_k = i) P(R_k = i) \\ &= \sum_{i=-C_{T_{ACK}}}^{\beta - C_k} P(U_T \geq C_k - i | R_k = i) P(R_k = i). \quad (4.21) \end{aligned}$$

Next we derive the P(success after outage) again using Equation (4.16) as

$$\begin{aligned} P(\text{success after outage}) &= P(E_{k+1} \geq C_k) \\ &= P(E_{k+1} \geq C_k | R_k = 0) P(R_k = 0) \\ &= P(U_{t_{out}} \geq C_k | R_k = 0) \\ &= P(U_{t_{out}} \geq C_k). \end{aligned} \tag{4.22}$$

4.2.2.1. Minimum Battery Capacity. As explained before when the transmitter receives an ACK it deduces $R_{k-1} = -C_{T_{ACK}}$ therefore Equation (4.21) will be simplified to

$$P(\text{success after transmission}) = P(U_T \geq C_k). \tag{4.23}$$

And success probability after an energy outage as

$$P(\text{success after outage}) = P(U_T \geq C_k - C_{T_{ACK}}). \tag{4.24}$$

4.2.2.2. Finite Battery Capacity. In this case of the blind communication with ACK, we can find a numerical solution to the PMF of the E_{ss} and we will use this PMF to find the P(success after ACK). So we can express the P(success after ACK) as

$$P(\text{success after ACK}) = \sum_{u=C_k}^{\beta} f_{E_{ss}}(u). \tag{4.25}$$

The outage case is the same as the minimum battery case because the transmitter learns $R_k = 0$ so we use Equation (4.11) to find success rate.

4.2.2.3. Infinite Battery Capacity. In the infinite battery capacity case we get rid of the battery constraint therefore Equation (4.25) changes to

$$P(\text{success after ACK}) = \sum_{u=C_k}^{\infty} f_{E_{ss}}(u). \tag{4.26}$$

In the outage event, we use Equation (4.12).

4.3. The ESI Communication

In the ESI communication protocol, the battery level of the receiver is formulated as

$$E_k = \max(\beta, R_{k-1} + U_\tau), \qquad \tau \in \{t_{wait_i}, t_{out}, T\},\ k \in 1, 2 \ldots . \tag{4.27}$$

The primary distinction from Equation (4.13) lies in the addition of t_{wait_i}, which represents the harvesting duration following the receipt of the ESI. The variable i in the t_{wait_i} changes in response to different ESI feedbacks. The residual energy R_k can be expressed as

$$R_k = \begin{cases} \max(E_k - C_k, -C_{T_{ACK}}) & \text{if } E_k \geq C_{T_{ESI}} + C_{R_{pckt}} \\ \max(E_k - C_k, 0) & \text{else.} \end{cases} \tag{4.28}$$

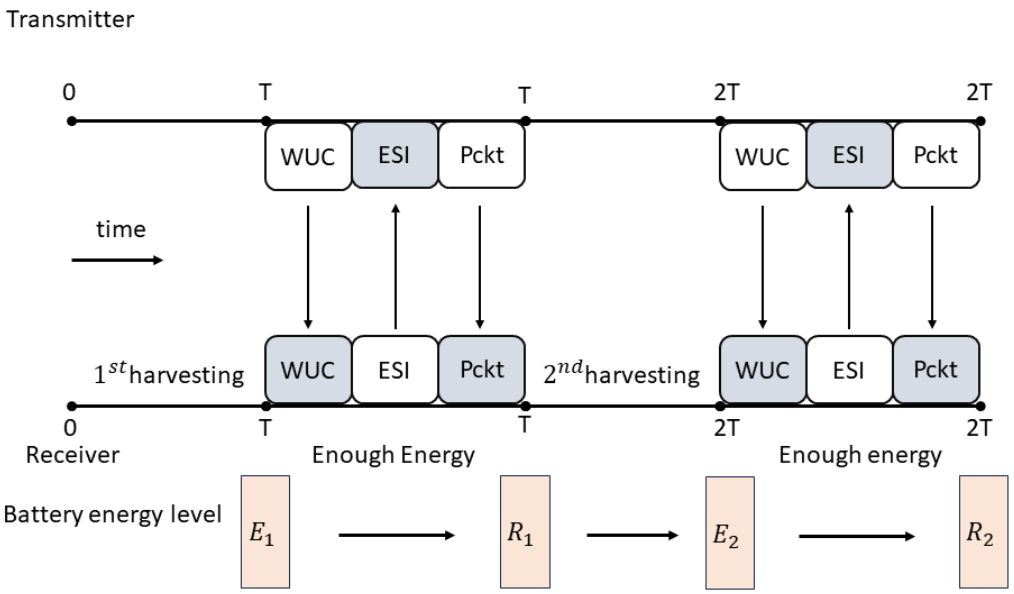

Figure 4.9. Packet transmission and battery energy level when the receiver has enough energy in the ESI communication.

Unlike other protocols, in the ESI communication protocol, C_k varies depending on the specific step in the communication process. We can express C_k as

$$C_k = \begin{cases} C_{T_{ESI}} + C_{R_{pckt}} + C_{T_{ack}} & \text{if direct reception} \\ C_{T_{ESI}} & \text{if the ESI not enough} \\ C_{R_{pckt}} + C_{T_{ack}} & \text{if after wait reception.} \end{cases} \tag{4.29}$$

Direct reception takes place when the ESI feedback indicates to the transmitter that the receiver possesses adequate energy which is shown in Figure 4.9. This allows the transmitter to send the packet immediately, eliminating the need for any waiting period. In contrast, if the ESI represents insufficient energy, the transmitter will not send the data packet. Upon receiving this ESI, the transmitter does not request the ESI again; instead, it proceeds to transmit its packet after t_{wait} duration this case is illustrated in Figure 4.10. The case for the reception fails after the waiting period is shown in Figure 4.11.

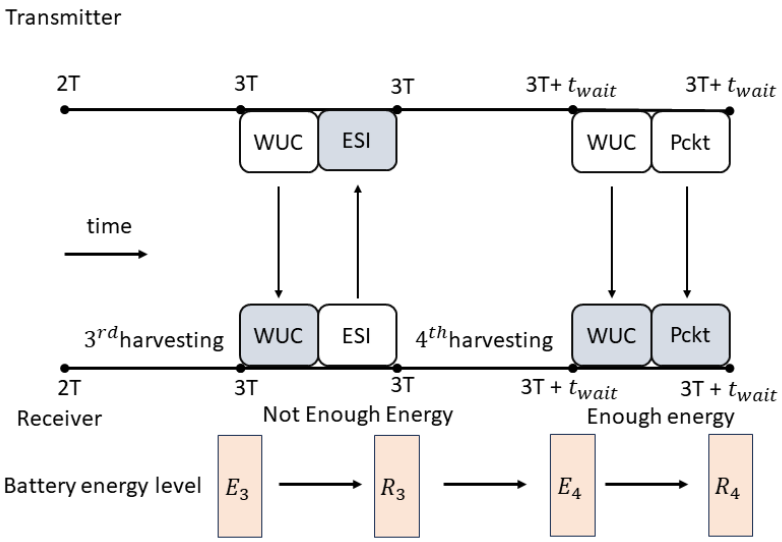

Figure 4.10. Packet transmission and battery energy level when the receiver does not have enough energy initially but after t_{wait} time reception completes in the ESI communication.

4.3.1. Energy Level Prediction

To avoid unnecessary energy expenditure, the transmitter requires ESI from the receiver node. Upon receiving the ESI, the transmitter acts accordingly. If the receiver

has sufficient energy, the transmitter sends the data packet; otherwise, the transmitter calculates t_{wait} and gives time to the receiver to harvest energy. Then transmits its packet after the waiting period ends.

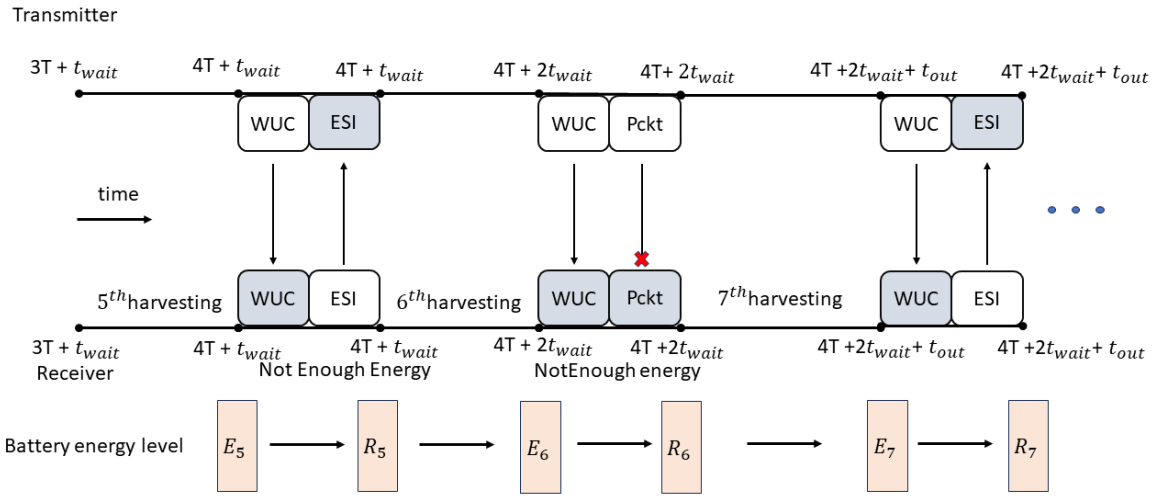

Figure 4.11. Packet transmission and battery level when the receiver does not have enough energy and after t_{wait} time receiver still does not have enough energy and goes to energy outage afterward transmitter waits t_{out} time in the ESI communication.

ESI essentially represents a quantized measurement of the battery level. The quantization of the battery level is crucial for two primary reasons. Without quantization, transmitting an ESI would lead to higher energy consumption, as it necessitates sending more bits. Additionally, calculating a precise ESI would increase the energy usage of the receiver and require a more complex receiver processor [30]. ESI can be expressed as

$$\text{ESI} = \begin{cases} 2^n & E_k \geq C \\ l & l \cdot C/(n-1) \leq E_k < (l+1)C/(n-1), \end{cases} \tag{4.30}$$

n represents the number of bits used to quantize the battery level, $C = C_{T_{ESI}} + C_{R_{pckt}}$ and l is the quantized value of the ESI. We distribute $2^n - 1$ energy levels uniformly within the interval $[0, 1, \ldots, C-1]$. The highest energy level 2^n corresponds to energy values greater than the total energy cost. ESI serves to approximate the residual energy in the receiver's battery at the end of a communication cycle, providing a baseline for

the next harvesting period. Consequently, we can determine the PMF of the E_{k+1} as

$$f_{E_{k+1}|\text{ESI}} = \begin{cases} f_{R_k|\text{ESI}} * f_{U_{t_{wait}}} & \text{if } E_{k+1} < \beta \\ 1 - F_{E_{k+1}|ESI}(\beta - 1) & \text{if } E_{k+1} = \beta \\ 0 & \text{if } E_{k+1} > \beta. \end{cases} \tag{4.31}$$

4.3.1.1. Minimum Battery Capacity. In the scenario of minimum battery capacity, the receiver's battery is only sufficient to cover the energy requirements for waking up, transmitting an ESI, and receiving a data packet. The transmission of an ESI occurs either when a data packet is ready to be sent or following an energy outage. In the former case $R_{k-1} = -C_{T_{ack}}$ and in the latter, $R_{k-1} = 0$. Upon receiving an the ESI less than 2^n transmitter calculates the PMF of E_k using Equations (4.27), and (4.30) and it is expressed as

$$\begin{aligned} f_{E_k|\text{ESI}}(e_k|\text{ESI} = l) &= \begin{cases} \dfrac{f_{U_{t_{out}}}(e_k)}{F_{U_{t_{out}}}((l+1)C/(n-1)) - F_{U_{t_{out}}}(l \cdot C/(n-1))} & \text{if outage} \\ \dfrac{f_{U_T}(e_k + C_{T_{ACK}})}{F_{U_T}((l+1)C/(n-1)) - F_{U_T}(l \cdot C/(n-1))} & \text{if ACK} \end{cases} \\ e_k &\in \left\{ \left\lceil \frac{l \cdot C}{n-1} \right\rceil, \ldots, \left\lceil \frac{(l+1)C}{n-1} \right\rceil \right\}. \end{aligned} \tag{4.32}$$

PMF of the R_k can be derived from Equation (4.28) as

$$f_{R_k|\text{ESI}}(e_k|\text{ESI} = l) = f_{E_k|\text{ESI}}(e_k + C_k|\text{ESI} = l). \tag{4.33}$$

This is because the energy cost for ESI transmission is deterministic and effectively shifts the probability distribution function to the left. Finally, the PMF of E_{k+1} with ESI can be estimated as

$$f_{E_{k+1}|\text{ESI}}(e_{k+1}|\text{ESI} = l) = \begin{cases} f_{E_k|\text{ESI}}(e_k + C_k|\text{ESI} = l) * f_{U_{t_{wait_l}}} & \text{if } E_{k+1} < \beta \\ 1 - F_{E_{k+1}|out}(\beta - 1) & \text{if } E_{k+1} = \beta \\ 0 & \text{if } E_{k+1} > \beta. \end{cases} \tag{4.34}$$

4.3.1.2. Finite Battery Capacity. In this case, we need to adjust Equation (4.32) because in the minimum case, there will not be any residual energy after a reception therefore Equation (4.32) changes to

$$f_{E_k|\text{ESI}}(e_k|\text{ESI}=l) = \begin{cases} \dfrac{f_{U_{t_{out}}}(e_k)}{F_{U_{t_{out}}}((l+1)C/(n-1)) - F_{U_{t_{out}}}(l\cdot C/(n-1))} & \text{if outage} \\ \dfrac{\sum_r f_{U_T}(e_k + C_{T_{ACK}} - r)\cdot f_{R_{k-1}}(r)}{\sum_{e_k}\sum_r f_{U_T}(e_k + C_{T_{ACK}} - r)\cdot f_{R_{k-1}}(r)} & \text{if ACK,} \end{cases}$$

$$e_k \in \left\{ \left\lceil \frac{l\cdot C}{n-1} \right\rceil, \ldots, \left\lceil \frac{(l+1)C}{n-1} \right\rceil \right\}. \tag{4.35}$$

So the estimation of the PMF of the E_{k+1} is done as same as Equation (4.34). In the ESI case the PMF varies with the reception of the ESI and ACK therefore the the PMF does not converge however due to ESI, PMFs that vary according to k after the same situations are sufficiently close to each other. The mentioned situations are after the same ESI value outcomes l or outage event. So the PMF that will be used to determine the P(success) is shown as

$$f_{E_{k+1}|ESI}(e_{k+1}|ESI=l) = \frac{\sum_r f_{U_T}(e_{k+1}-r)\cdot f_{U_{t_{wait}}}(r)}{\sum_{e_k}\sum_r f_{U_T}(e_{k+1}-r)\cdot f_{U_{t_{wait}}}(r)},$$
$$e_k \in \left\{ \left\lceil \frac{l\cdot C}{n-1} \right\rceil, \ldots, \left\lceil \frac{(l+1)C}{n-1} \right\rceil \right\}. \tag{4.36}$$

4.3.1.3. Infinite Battery Capacity. The infinite battery case is the same as the finite battery case the only difference is that the battery constraints drop. Therefore we use Equation (4.36) to find the PMF of the next energy level.

4.3.2. Calculating the Harvesting Time

In this protocol, the transmitter sends data packets under three specific conditions. These conditions are specified as follows: upon receiving an ESI= 2^n after an acknowledgment, upon receiving an ESI= 2^n after an outage, upon receiving an ESI< 2^n than waiting to send packet. The probability of the transmitter realizing the first case (after an acknowledgment) is expressed as

$$P(\text{success after ACK}) = P(E_{k+1} \geq C)$$

$$
\begin{aligned}
&= \sum_{i=-C_{T_{ACK}}}^{\beta-C_k} P(E_{k+1} \geq C | R_k = i) P(R_k = i) \\
&= \sum_{i=-C_{T_{ACK}}}^{\beta-C_k} P(R_k + U_T \geq C | R_k = i) P(R_k = i) \\
&= \sum_{i=-C_{T_{ACK}}}^{\beta-C_k} P(U_T \geq C - i | R_k = i) P(R_k = i). \qquad (4.37)
\end{aligned}
$$

Similarly, the probability of the transmitter realizing the second case (after an outage) is expressed as

$$
\begin{aligned}
P(\text{success after outage}) &= P(E_{k+1} \geq C) \\
&= P(E_{k+1} \geq C | R_k = 0) P(R_k = 0) \\
&= P(R_k + U_T \geq C | R_k = 0) P(R_k = 0) \\
&= P(U_T \geq C - i | R_k = 0). \qquad (4.38)
\end{aligned}
$$

We have previously noted that when the transmitter receives an ESI less than $< 2^n$, it waits for a duration of t_{wait} before transmitting the packet. Consequently, the probability of success after this waiting period, denoted as $P(\text{success after ESI})$ can be expressed as

$$
\begin{aligned}
P(\text{success after ESI}) &= P(E_{k+1} > C | \text{ESI} = l) \\
&= \sum_{i=\lceil lC/(n-1) \rceil}^{\lceil (l+1)C/(n-1) \rceil - 1} P(E_{k+1} \geq C | R_k = i) P(R_k = i | \text{ESI} = l) \\
&= \sum_{i=\lceil lC/(n-1) \rceil}^{\lceil (l+1)C/(n-1) \rceil - 1} P(R_k + U_{t_{wait}} \geq C | R_k = i) P(R_k = i | \text{ESI} = l) \\
&= \sum_{i=\lceil lC/(n-1) \rceil}^{\lceil (l+1)C/(n-1) \rceil - 1} P(U_{t_{wait}} \geq C - i | R_k = i) P(R_k = i | \text{ESI} = l). \qquad (4.39)
\end{aligned}
$$

4.3.2.1. Minimum Battery Capacity. When the battery capacity is $C_{R_{pckt}} + C_{T_{ESI}}$ as explained in the previous protocol Equation (4.37) simplifies due to the battery capacity being too low to store residual energy. Therefore success rate after receiving and ACK can be expressed as

$$
P(\text{success after ACK}) = P(U_{t_{out}} \geq C + C_{T_{ACK}} | R_k = -C_{T_{ACK}}), \qquad (4.40)
$$

and Equation (4.38) simplifies to

$$P(\text{success after outage}) = P(U_{t_{out}} \geq C | R_k = 0), \tag{4.41}$$

and lastly Equation (4.39) simplifies to

$$P(\text{success after ESI}) = \sum_{i=\lceil lC/(n-1) \rceil}^{\lceil (l+1))C/(n-1) \rceil - 1} P(U_{t_{wait}} \geq C - i | R_k = i) f_{R_k|\text{ESI}}(i). \tag{4.42}$$

4.3.2.2. Finite Battery Capacity. In the case of a finite battery limit, the residual energy in the battery complicates the calculations and adds a dependency on the previous energy level of the battery. However because ESI eliminates some of the uncertainty the transmitter can estimate the previous energy level with Equation (4.35) and to find the success target under different feedback receptions we can insert Equation (4.35) into the Equations (4.38), and (4.39).

4.3.2.3. Infinite Battery Capacity. In the infinite battery scenario, we adhere to the same procedures as in the finite battery case, since the primary complexity arises from the residual energy in the battery. The only difference between the finite and infinite battery scenarios is that the battery capacity constraints are disregarded in the infinite battery case.

5. RESULTS

In the previous chapters, we derived the necessary formulas for energy harvesting then protocols are througly explained and energy consumption charecteristics of the protocols are noted. Lastly we investigated the energy level of the receiver during operation and closed-form solutions to PMF of energy levels and P(success) are calculated for all battery capacity cases and the three proposed protocols. In this section, we will observe the effects of the harvesting times to the performance metrics of the protocols.

Our calculations were conducted with both time and energy discretized. The discrete time steps were set at 1-second (s) intervals, and the discrete energy steps were established at increments of 1 mJ. The T is set for different values to see its relation with the other harvesting times. Also, the simulations have been conducted for a period corresponding to 1.5 years and a minimum number of receptions is more than 300 thousand. The values used in the simulations are shown in Table 5.1 the energy packet arrival rate λ is adapted from the article [31].

Table 5.1. Parameters used in the simulation.

Parameters	Values
λ	0.15
X_i	1 mJ
$C_{R_{pckt}}$	12 mJ
$C_{T_{ack}}$	1 mJ
$C_{T_{ESI}}$ 1bit ESI	1 mJ
$C_{T_{ESI}}$ 2bit ESI	2 mJ
Packet length (l)	2 kb
Transmission rate	20 kbps

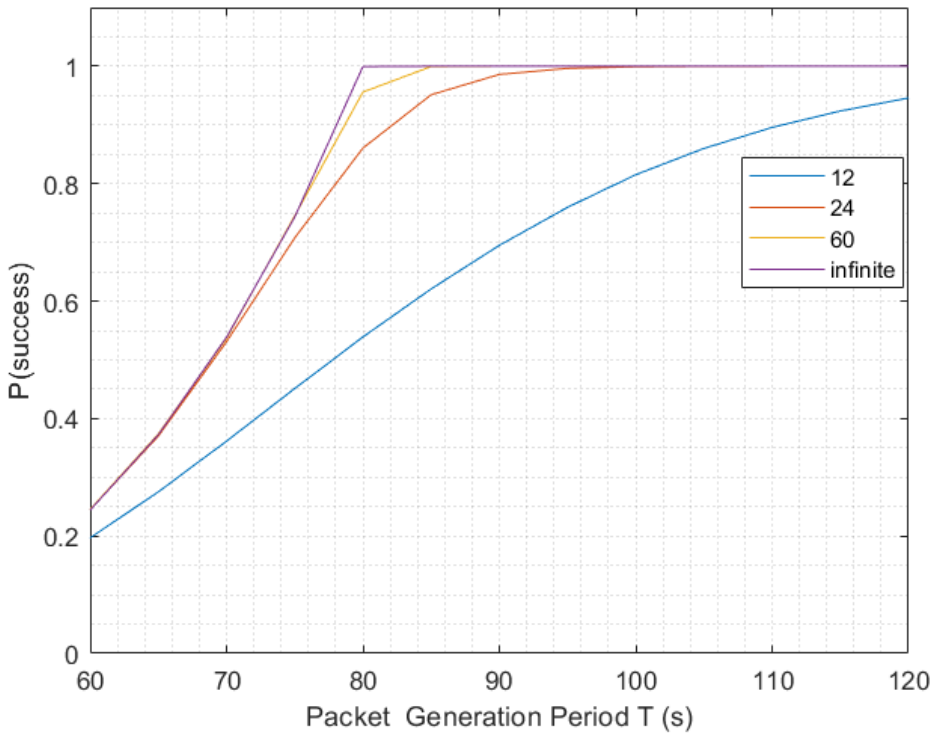

Figure 5.1. The effect of T on the P(success) with varying battery capacities for blind communication without ACK.

5.1. The Blind Communication without ACK

In this section, we investigate the impact of the packet period T's impact on several key parameters: the probability of successful communication P(success), and the average time between receptions under the minimum battery capacity case. In Figure 5.1 we observe that battery capacity affects the P(success). Probabilistically in some harvesting durations, because more energy than C_k is collected, the amount of energy in the battery increases. Therefore, even if the receiver cannot collect sufficient energy in the following harvesting durations, it can still successfully receive the packet by using the energy in the battery.

When the data generation period is equal to the 80 s, see that in the infinite battery case outage probability goes to 0. The importance of the 80 s mark stems from the fact that the average energy harvested over 80 s equals the energy consumed during the packet reception. Therefore in the mean sense receiver would have enough

energy to receive packets. With usage of an infinite battery outage probability goes to 0 when mean power and consumptions are equal which is explained in the [29] This phenomenon, where the transmitter aligns its packet generation period with the receiver's mean harvesting power, will be referred to as the transmitter matches the packet generation period with the receiver's harvesting power.

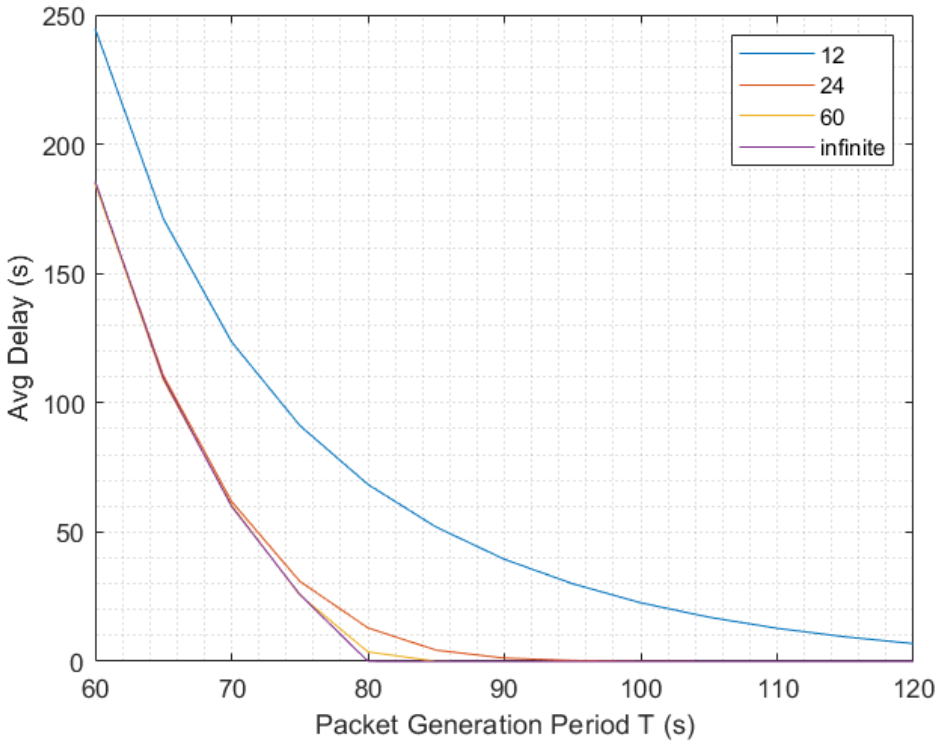

Figure 5.2. The effect of T on the average delay time with varying battery capacities for blind communication without ACK.

The average delay time parameter indicates the difference between the moment the transmitter wants to send the packet and the moment the receiver successfully receives it. It is important to highlight that we ignore the propagation, processing, and transmission delays these delays are very small compared to the energy harvesting times. In Figure 5.2, it is observed that as the harvesting duration increases, the average delay decreases. This phenomenon was similarly noted in Figure 5.1, where the outage probability decreases, and eventually, the average delay converges to 0. Additionally, the battery capacity serves as an outage protection buffer, further reducing both the outage probability and the average delay time.

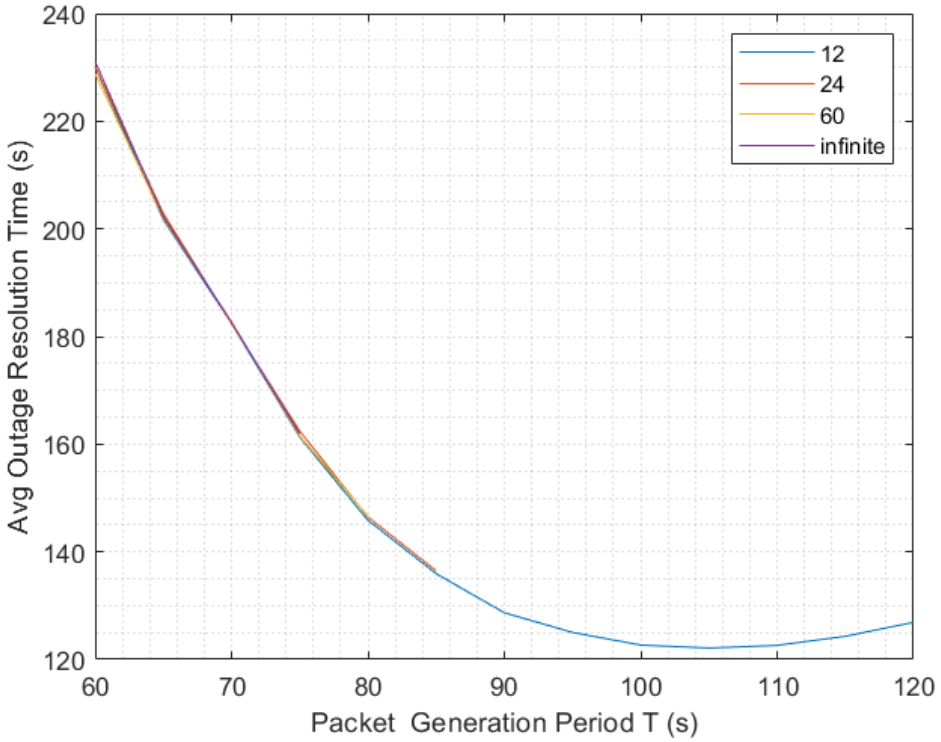

Figure 5.3. The effect of T on the average outage resolution time with varying battery capacities for blind communication without ACK.

The average outage resolution time indicates how long it takes for a packet to be received after an outage event. This parameter is a decisive indicator for applications where the delay time is important. Figure 5.3 demonstrates that as the harvesting duration increases, the average outage resolution time decreases until it reaches a minimum at $T = 105$ s for the case of the minimal battery capacity. This decrease occurs because, up to $T = 105$ s point, the outage probability is relatively high, leading to frequent consecutive outage events which increases the time between successful receptions. Beyond $T = 105$ s, the outage probability decreases, suggesting that the receiver has adequate time to harvest enough energy. However, this also results in the transmitter waiting excessively long to send the packet, despite the receiver having sufficient energy, causing an increase in the average outage resolution time. In scenarios with higher battery capacities, the number of outage events significantly decreases because $P(\text{success})$, converges to one very rapidly there fore higher T values are not added to the graph.

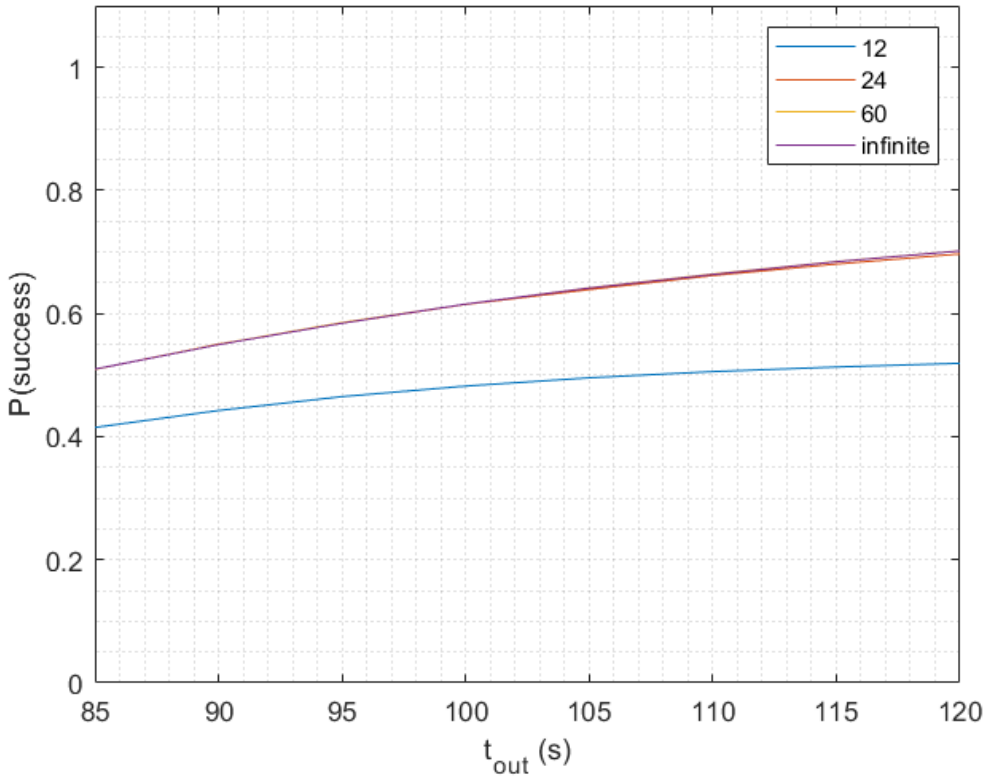

Figure 5.4. The effect of t_{out} on the P(success) for varying battery capacities for blind communication with ACK when $T = 60$ s.

5.2. The Blind Communication with ACK

In this protocol, we investigate the effects of t_{out}, β, and T on the parameters of P(success), average delay time, and average outage resolution time. Therefore, three packet generation periods, T's (60 s, 75 s, 90 s), are examined under different β's (12 mJ, 24 mJ, 60 mJ, infinite) and t_{out}'s. In Figures 5.4, 5.5, and 5.6, we observe that as T increases, P(success) also increases, as similar to the previous protocol. Here, we also note that especially in Figure 5.4 increase in t_{out} enhances the system's outage performance, especially when the battery capacity is high. However, the effect of t_{out} becomes somewhat insignificant as the packet generation period increases. This is because, with an increase in T, the receiver can harvest more energy, resulting in a decrease in the number of outage events and rendering the impact of t_{out} insignificant in comparison to all receptions.

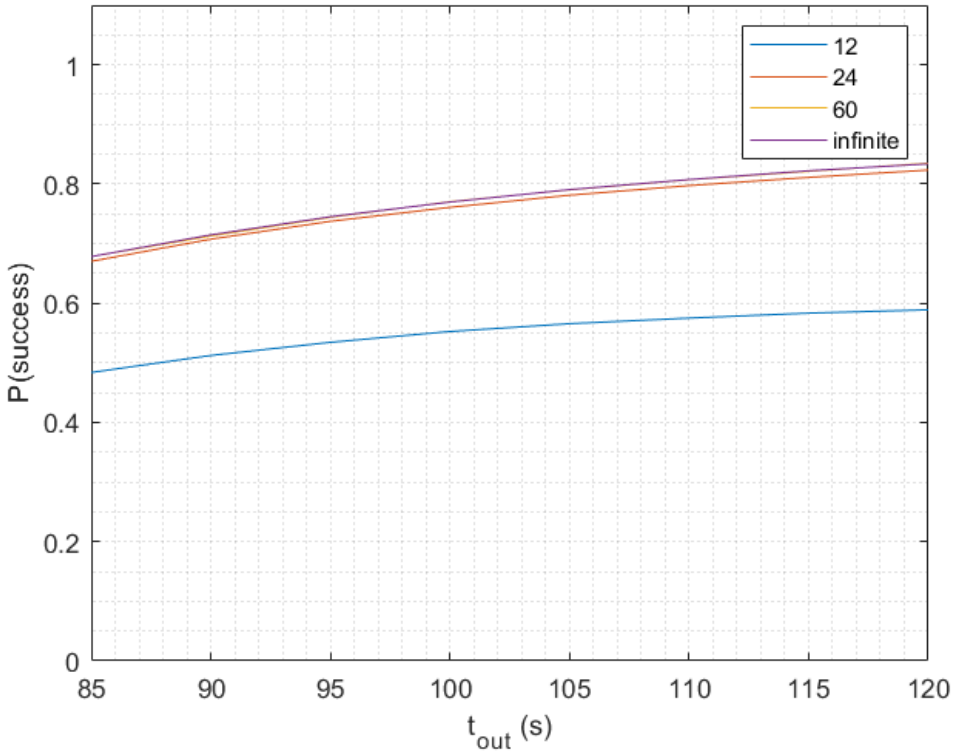

Figure 5.5. The effect of t_{out} on the P(success) for varying battery capacities for blind communication with ACK when $T = 75$ s.

The energy cost for packet reception and transmitting an ACK is 13 mJ. On average, the receiver requires approximately 85 s to harvest enough energy to receive a packet successfully, making it potentially unreasonable to send data more frequently than 85 s. Nevertheless, we aim to explore the system's behavior under low-power conditions so increasing the frequency of data generation gives a good insight. Also in many WSN scenarios, the receiver's only energy consumption does not stem from receiving packets from a dedicated transmitter. Hence, the transmitter may not be aware of the receiver's energy consumption patterns. To address this, we also examine low packet generation periods to understand the protocol's behavior amid frequent outage events. In Figure 5.5, we observe that an increase in t_{out} enhances the P(success) because it acts as a negative feedback mechanism when T is lower than packet generation matched period. The use of ACK prevents the transmitter from overloading the receiver harvesting capacity with frequent packet transmission, which in turn aids in improving the overall success rate.

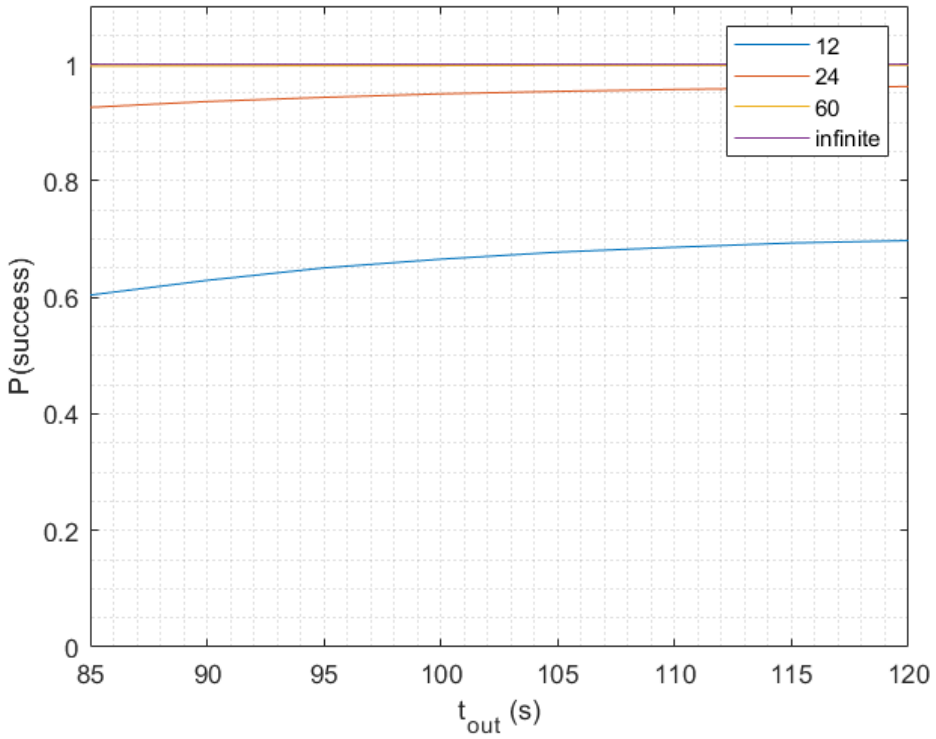

Figure 5.6. The effect of t_{out} on the P(success) for varying battery capacities for blind communication with ACK when $T = 90$ s.

When the packet generation interval surpasses the average duration needed to power the receiver as in Figure 5.6, it clearly results in an increased success rate. As observed in the previous protocol, the battery capacity plays a crucial role in enabling the receiver to attain a zero outage probability. In this scenario, with the outage probability being exceedingly low, employing ACK becomes redundant since the transmitter can be almost certain of packet reception. This renders the energy expended on transmitting ACK superfluous, particularly in scenarios with high battery capacity and packet generation periods.

In Figures 5.7, 5.8, and 5.9, we examine the behavior of the average delay time in relation to t_{out} across various battery scenarios and packet generation periods. While a non-increasing trend is observed with larger battery capacities, a distinct minimum point emerges in the case with minimal battery capacity. This pattern is akin to the phenomenon where, as T becomes excessively long, the average delay increases. This increase in delay is because of the transmitter waiting too long to send data, thereby

degrading performance by energy due to the battery overcharging therefore wasting harvested energy. However, this effect is not evident in scenarios with larger battery capacities, as the energy harvested during extended periods is stored in the battery. This stored energy is then available to mitigate potential outage events, effectively preventing them.

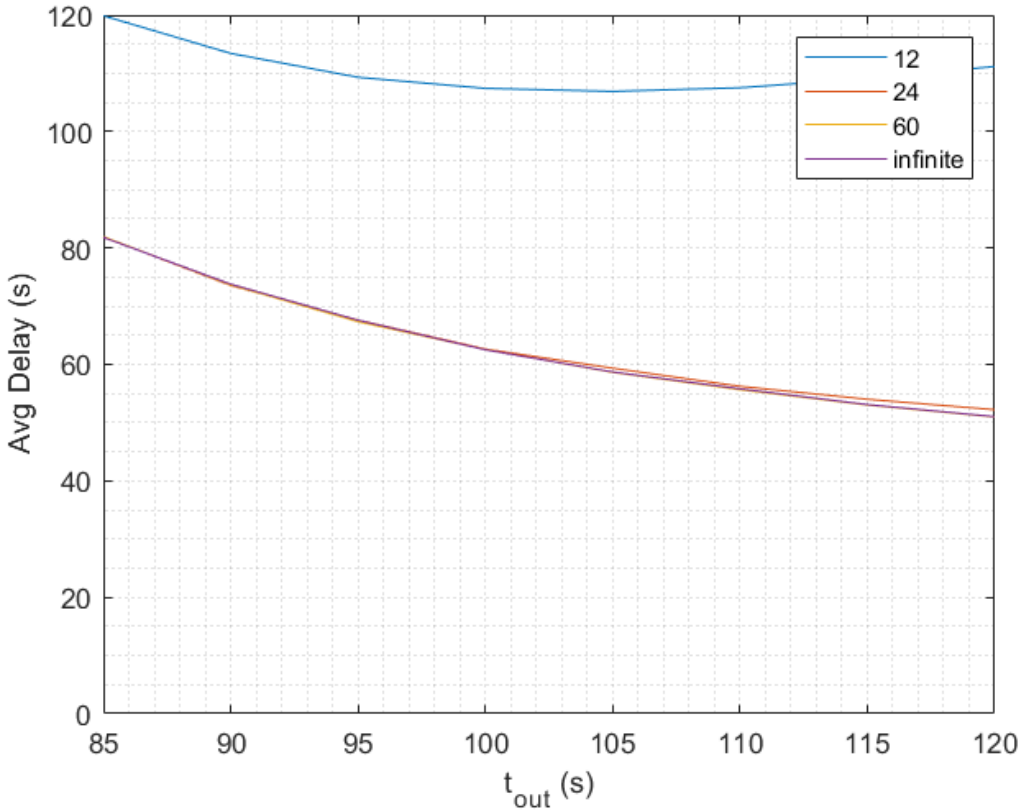

Figure 5.7. The effect of t_{out} on average delay time for varying battery capacities for blind communication with ACK when $T = 60$ s.

In Figure 5.7, we observe a significant decrease in the average delay when the battery capacity is increased from 12 mJ to 24 mJ. However, further increasing the battery capacity (to 60 mJ or infinite) has a negligible effect. This is attributed to the data generation period being too short for the receiver to reach an overcharging condition, so even a 24 mJ battery effectively is as large as an infinite one. Consequently, in scenarios where the receiver has limited time to harvest energy, a large battery capacity is unnecessary.

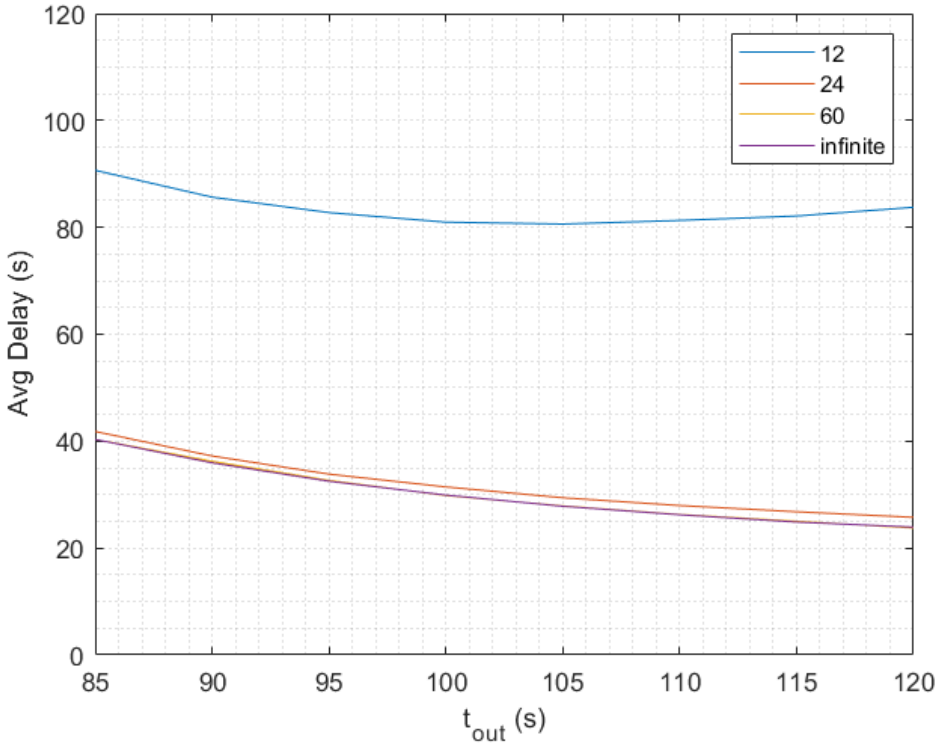

Figure 5.8. The effect of t_{out} on average delay time for varying battery capacities for blind communication with ACK when $T = 75$ s.

In Figures 5.8, and 5.9, the positive impact of battery capacity on the system's average delay becomes more pronounced as the packet generation time increases. This improvement is due to the increased likelihood that the receiver can store excess harvested energy in the battery, and the additional energy available prevents the system from entering an outage state, thereby significantly reducing the delay. Furthermore, higher t_{out} values assist the receiver in storing energy after an outage event for future receptions, which also contributes to a decrease in the average delay.

In Figure 5.9, we observe again that zero outage events are achieved for battery capacities of 60 mJ and infinite. However, due to the energy cost associated with transmitting ACK, the average delay metric does not perform as well as it does in blind communication without ACK. This underscores the redundancy of using ACK in situations where their contribution to improving system performance is outweighed by their energy costs.

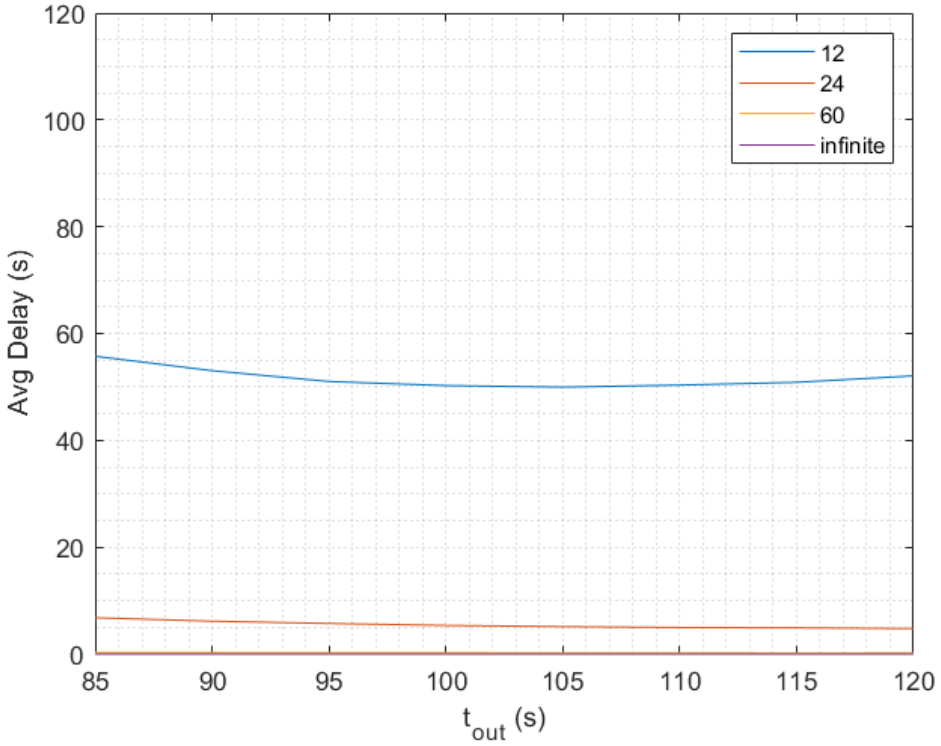

Figure 5.9. The effect of t_{out} on average delay time for varying battery capacities for blind communication with ACK when $T = 90$.

For the average outage resolution time parameter, Figure 5.10 shows that battery capacity does not significantly influence this metric. This is because an outage indicates that the receiver has already depleted its stored energy and must start harvesting energy from scratch, rendering the battery capacity irrelevant in this context. Additionally, the packet generation period T also does not impact this parameter, as indicated in the figures. After an outage event, the recovery time is not directly affected by T. Thus, the only parameter that effectively influences the outage resolution time is t_{out}.

5.3. The ESI Communication

In this protocol, we examine the impact of t_{wait}, β, and T on the outcomes of P(success), average delay time, and average outage resolution time. We set t_{out} to 105 s across the following simulations, as indicated by Figure 5.10, where it's shown to minimize the average outage resolution time. It's crucial to note that the choice of t_{out} has minimal impact when the outage probability is low. Our primary objective

in this protocol is to prevent sending packets to the receiver when it lacks sufficient energy, thus significantly reducing the number of outage events even during short packet generation periods.

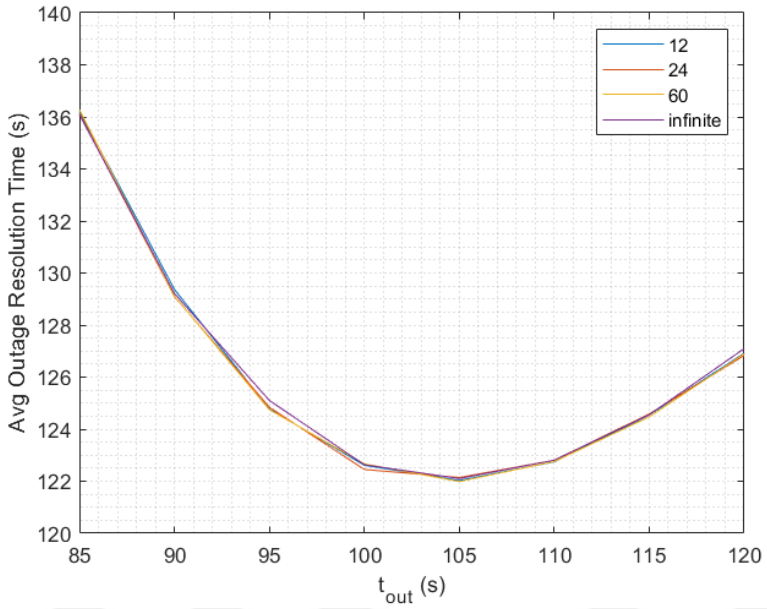

Figure 5.10. The effect of t_{out} on the average outage resolution time for the different battery capacities for blind communication with ACK when $T = 60$ s.

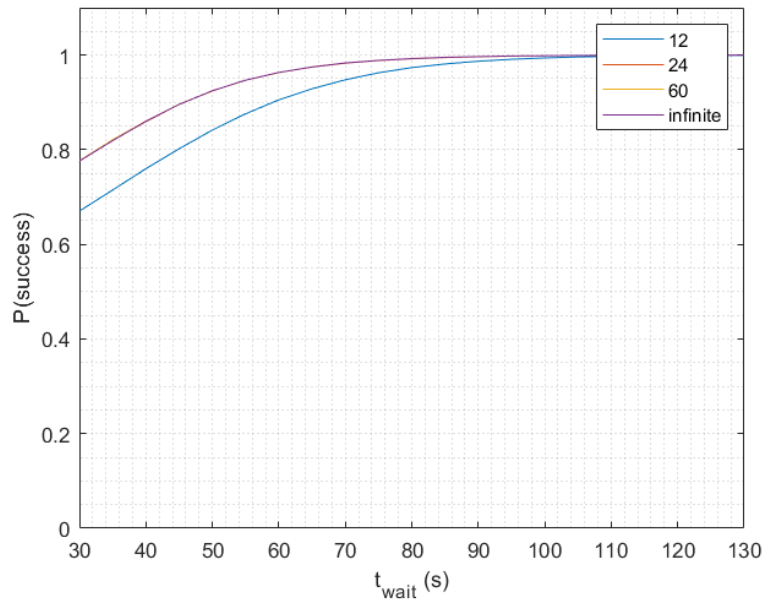

Figure 5.11. The effect of t_{wait} on the P(success) for varying battery capacities for blind communication with ACK when $T = 60$ s.

In Figures 5.11, 5.12, and 5.13, we observe that the use of Energy Status Information (ESI) enhances the overall success rate compared to previous protocols. The transmitter, informed about whether the receiver has adequate energy, waits for t_{wait} if the receiver's energy is insufficient, allowing more time for energy harvesting. This straightforward strategy substantially lowers the outage probability, as illustrated in the figures.

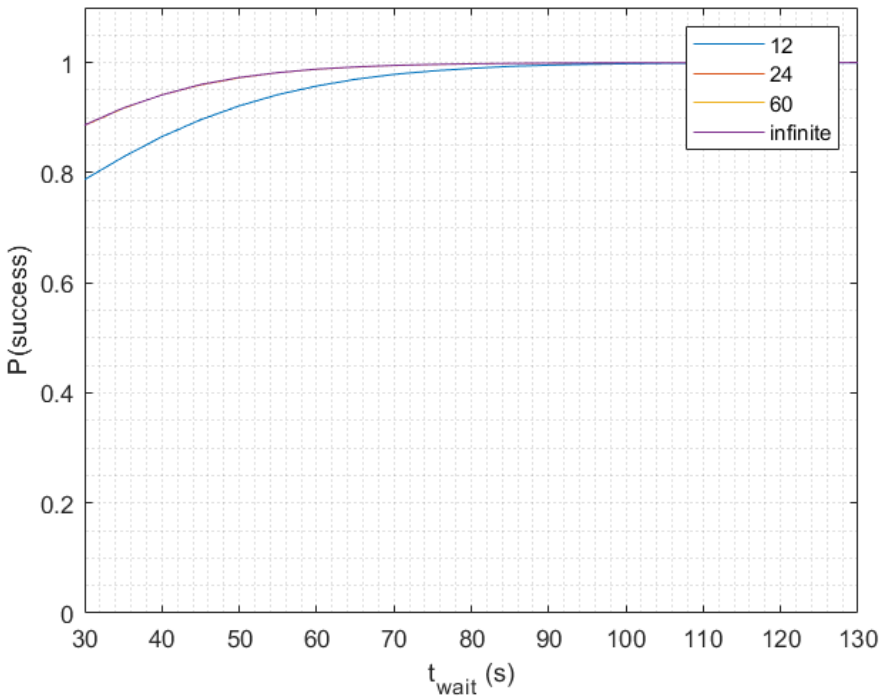

Figure 5.12. The effect of t_{wait} on the P(success) for varying battery capacities for ESI communication when $T = 75$ s.

The downside of analyzing this parameter is that the energy cost of transmitting ESI and ACK is not clear in this parameter as it is observed in Figure 5.12 the outage probability converges to 0 eventually. Even in the $T = 90$ s packet generation period which is shown in Figure 5.13 the P(success) is not always 1 this is because the overall protocol consumes 14 mJ (12 mJ receiving the packet 1 mJ transmitting ESI and 1 mJ transmitting the ACK) therefore average needed time is 93 s which was only 80 s in the first protocol. Therefore in the blind communication cases the outage probability is always 0 for high battery capacity cases however here we see that low t_{wait} durations may result in energy outages therefore decreasing overall P(success).

Implying that while it improves certain aspects of the protocol, it introduces additional energy expenditures.

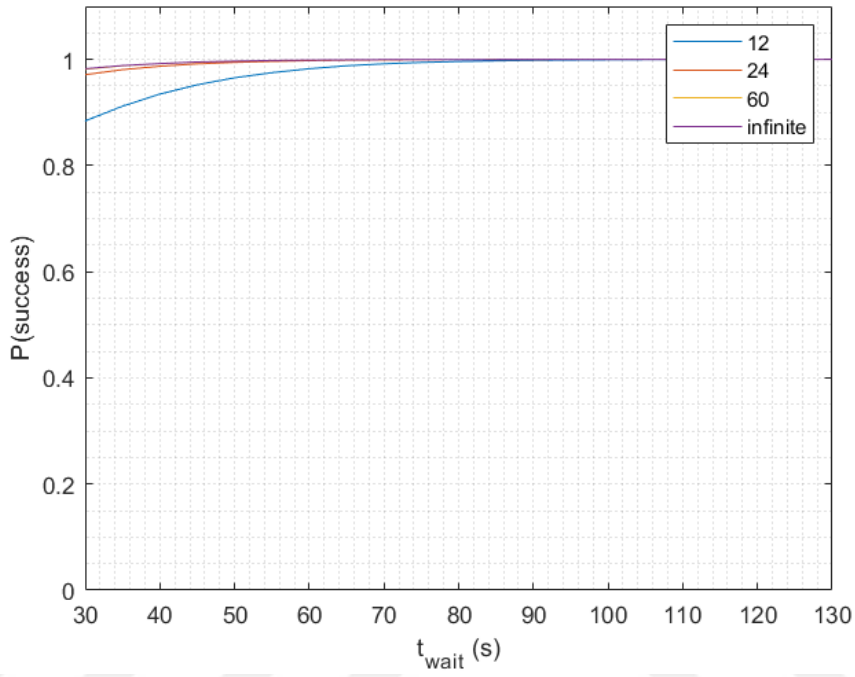

Figure 5.13. The effect of t_{wait} on the P(success) for varying battery capacities for ESI communication when $T = 90$ s.

In Figures 5.14, 5.15, and 5.16, we focus on the average delay parameter. Figure 5.14 illustrates that for battery capacities of infinite and 60 mJ, the average delay values converge to 33 s as t_{wait} increases. This convergence is attributed to the use of excess energy harvested during the waiting period for not just the next packet reception but also for future receptions. Consequently, the combined packet generation and average delay times (60 s + 33 s) align with the average time required to power the receiver (93 s). This finding is crucial as it demonstrates that through the application of ESI, the transmitter can achieve an optimal average packet reception rate, even if it cannot directly match the data generation period to the receiver's energy harvesting needs, provided the battery capacity is sufficiently large. This approach, especially when compared to the scenarios depicted in Figures 5.2, and 5.7, significantly minimizes the average delay, showcasing the effectiveness of ESI in improving communication efficiency between transmitter and receiver under various energy conditions.

The behavior of the system with the minimum battery capacity mirrors that observed in previous protocols. Initially, as t_{wait} increases, the outage probability decreases due to the additional time allowed for the receiver to harvest energy before attempting packet reception. However, after reaching a minimum point, the trend reverses, and the outage probability begins to increase again. This increase is attributed to the transmitter waiting unnecessarily long periods before sending packets, which, rather than optimizing energy use or improving reception rates, instead introduces inefficiencies into the system's operation.

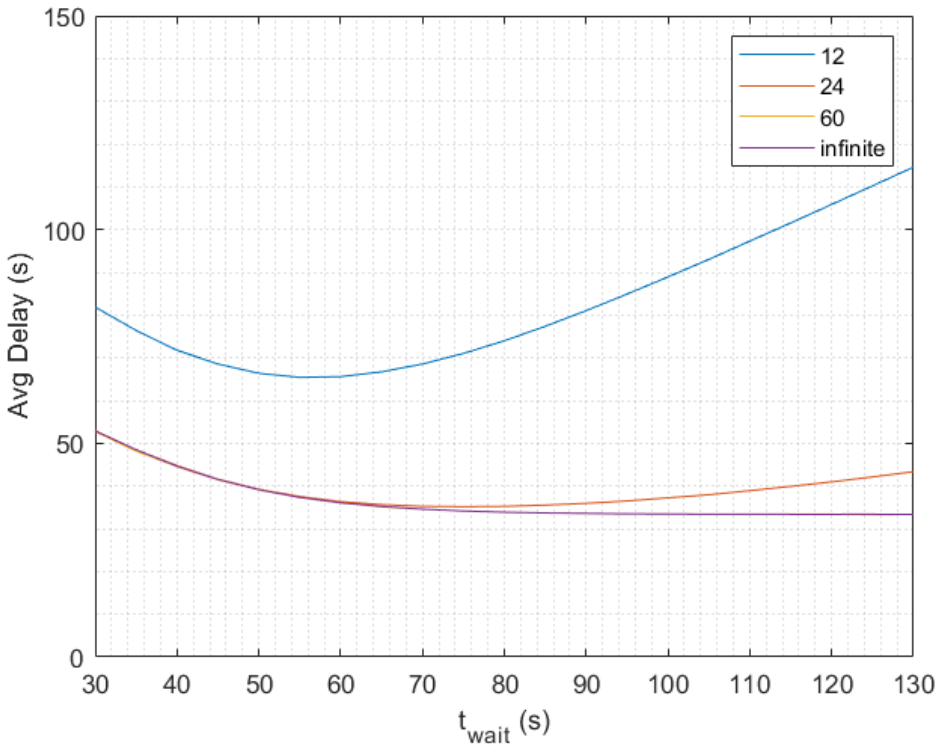

Figure 5.14. The effect of t_{wait} on the average delay time for varying battery capacities for blind communication with ACK when $T = 60$ s.

In Figure 5.15, where T is extended to 75 s, we again note our critical improvement: the average packet reception time converges to 93 s, as evidenced by the average delay time convergence at 18 s. In addition to that, increasing T reduces the significance of pinpointing the optimal t_{wait}, which in turn underscores the adaptability of our proposed protocol. This flexibility is particularly valuable in real-life energy harvesting systems, where the variability in energy availability can complicate the calculation of

the average time required to power the system. By adjusting either T or t_{wait}, our protocol effectively maximizes the number of packet receptions for the average case, achieving this with minimal complexity. This adaptability ensures robust performance even when faced with the inherent unpredictability of energy harvesting environments.

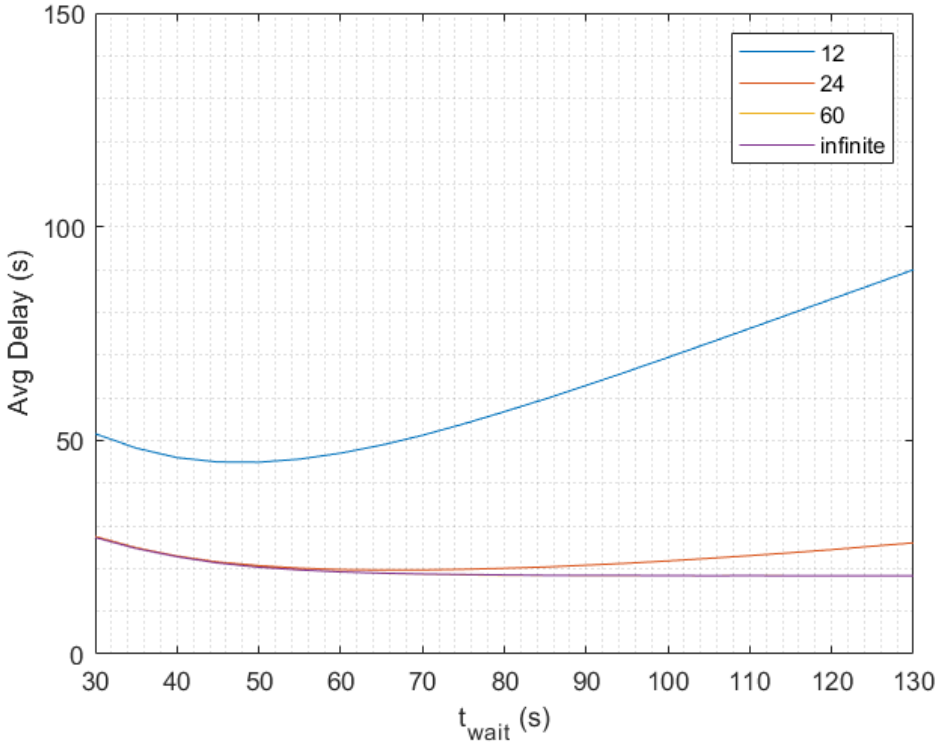

Figure 5.15. The effect of t_{wait} on the average delay time for varying battery capacities for ESI communication when $T = 75$ s.

In the final analysis of the average delay, with T set to 90 s, we observe a continuation of the previously mentioned behaviors: the alignment of the transmitter's packet transmission time with the receiver's energy harvesting time, along with the additional energy costs associated with the protocol, become apparent. In this scenario, whereas a 90 s interval was sufficient in previous protocols to achieve zero delay and zero outage Figure 5.2, and 5.9, such outcomes are not attainable in the current setup due to the energy costs incurred from transmitting the ESI and ACK. This highlights a critical trade-off in the protocol's design: while the inclusion of ESI and ACK mechanisms enhances the protocol's efficiency and reliability by ensuring energy adequacy before transmission, these features also introduce energy expenditures that impact the

system's ability to achieve the ideal scenario of zero delay and zero outage. This underscores the importance of carefully balancing protocol functionalities with their energy implications, especially in energy-constrained environments.

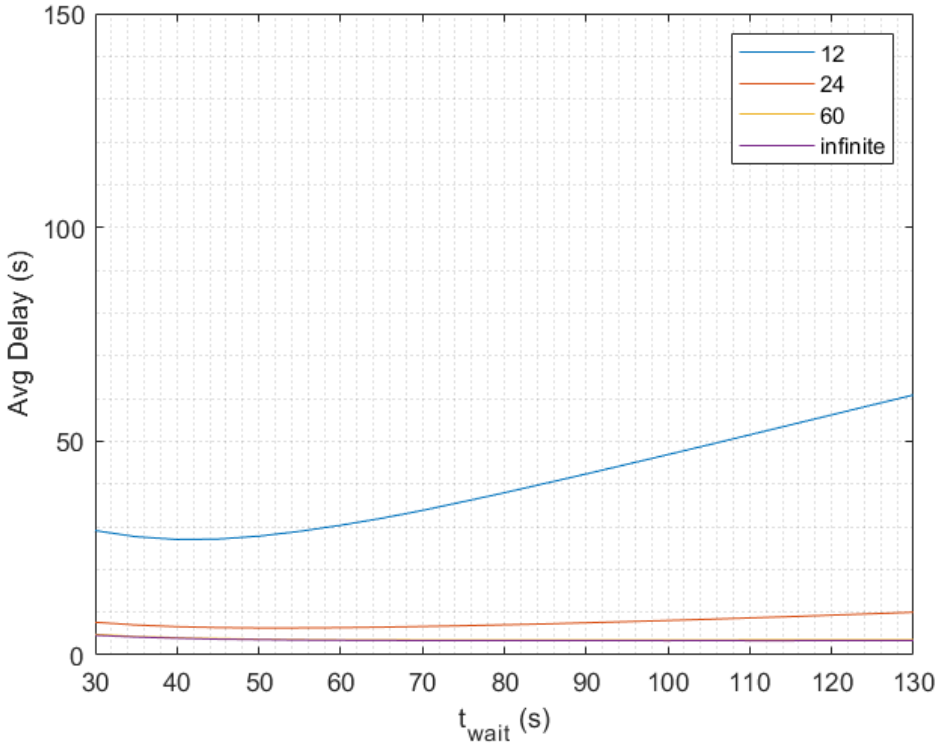

Figure 5.16. The effect of t_{wait} on the average outage resolution time for varying battery capacities for ESI communication when $T = 90$ s.

In Figures 5.17, and 5.18, we examine the average outage resolution time, a parameter that specifically addresses scenarios where the receiver lacks sufficient energy, leading to energy outages. In these cases, the receiver transmits ESI value of less than 2^n, prompting the transmitter to initiate a wait period (t_{wait}). Thus, the focus is solely on instances where the receiver's feedback indicates an energy deficit. This metric is crucial as it reflects the protocol's efficiency in recovering from disruptions, offering insights into the duration required to rectify situations where communication is compromised.

The introduction of ESI communication significantly enhances this performance metric compared to previous protocols. A lower t_{wait} may lead to retransmissions

triggered by energy shortfalls, as evidenced across all three figures. For instance, Figure 5.17 highlights a specific observation in the infinite battery case where the optimal t_{wait} of 50 s corresponds to an average outage resolution time of 66 s. This discrepancy suggests the occurrence of outages even with ESI transmissions. However, an increase in t_{wait} reveals a convergence between t_{wait} and the average outage resolution time. This alignment indicates that, with a sufficiently extended t_{wait}, the protocol effectively mitigates the issue of energy outages.

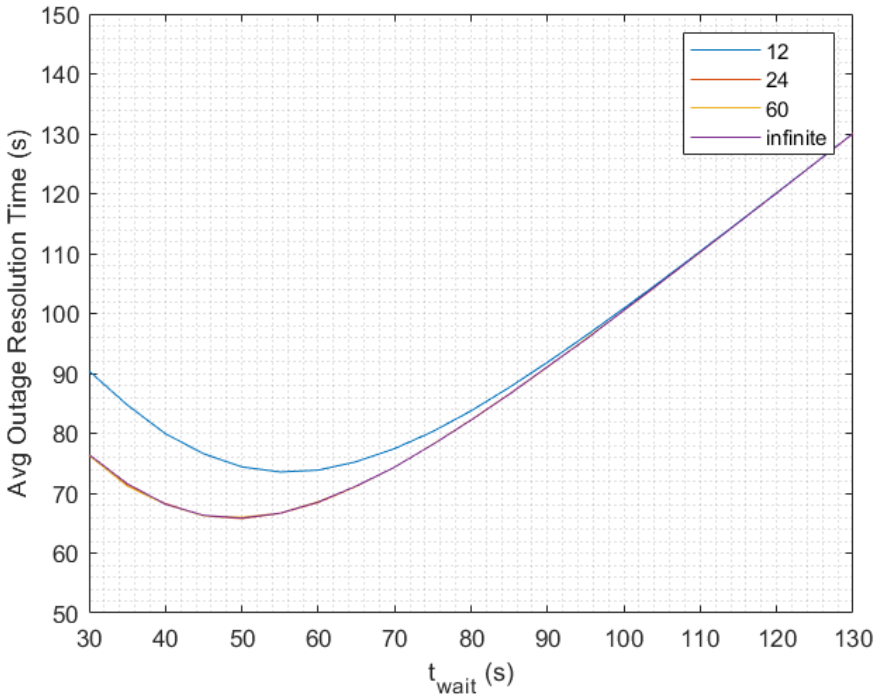

Figure 5.17. The effect of t_{wait} on the average outage resolution time for the different battery capacities for blind communication with ACK when $T = 60$ s.

We also observe the effect of the T on the average outage resolution in Figure 5.17, and 5.18. In the previous protocols, it was shown that the T does not affect the average outage resolution. The reason for this effect is that as T increases likely hood of the residual energy that was not enough to receive a packet actually closer to the needed energy. Which results less wait times needed to harvest energy shortage. Therefore increase in the T not only improves the success rate of the system but also improves the average outage resolution time.

In Figures 5.17, and 5.18, it's noted that the average outage resolution time is influenced by the battery capacity, a departure from previous protocols where battery capacity did not significantly impact this parameter. The reason for this difference lies in the operational dynamics of the ESI communication protocol. In earlier protocols, energy outages would lead the receiver to exhaust its energy reserves in the attempt to receive a packet. However, with ESI communication, the receiver utilizes a portion of its energy to signal that its energy level is insufficient for packet reception, rather than depleting its energy entirely in a failed reception attempt. This strategic use of energy means that, as the battery capacity increases, there's a likelihood of residual energy remaining in the battery even after an outage event.

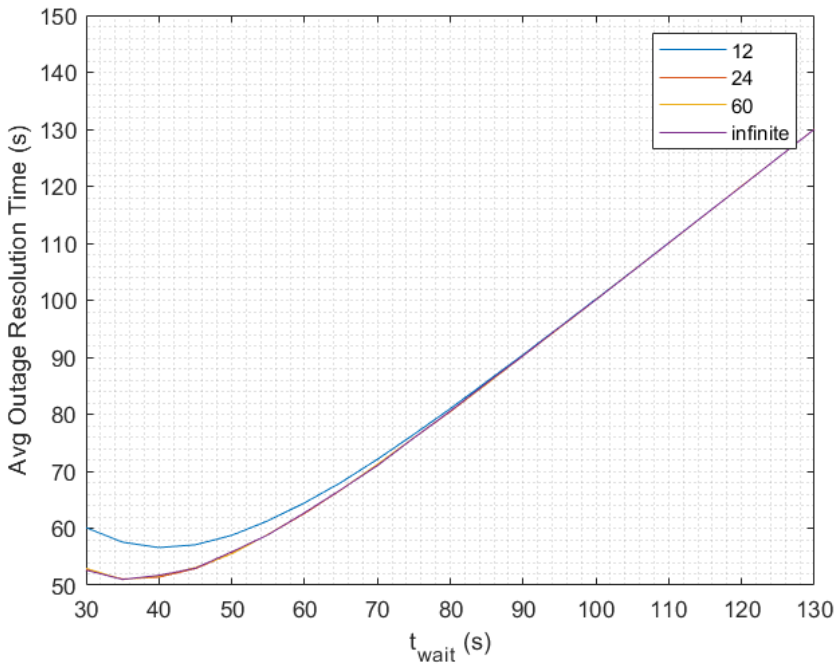

Figure 5.18. The effect of t_{wait} on the average outage resolution time for varying battery capacities for ESI communication when $T = 90$ s.

For battery capacities of 24 mJ, 60 mJ, and infinite, the receiver statistically has more leftover energy (R_k) and thus requires less additional energy to recover from an outage compared to scenarios with the minimum battery capacity. This nuanced behavior highlights the efficiency of ESI communication in managing energy resources more effectively, allowing for quicker recovery from outages in cases with higher battery capacities.

6. CONCLUSION

This thesis has explored the intricacies of WSN communication protocols under low-power energy harvesting, focusing on the optimization of packet transmission strategies to enhance system performance. Through detailed simulation studies, we investigated the effects of key parameters such as packet generation period (T), wait times (t_{wait} and t_{out}) on the probability of successful packet reception (P(success)), average delay time, and average outage resolution time. The findings provide valuable insights into the dynamics of energy-harvesting communication systems and propose practical strategies for improving reliability and efficiency. The introduction of ACK and ESI mechanisms was examined in depth, revealing their significant impact on system behavior. While ACK serves to confirm packet receptions, thereby reducing unnecessarily high frequent transmissions, ESI enables the transmitter to make informed decisions about transmission timing based on the receiver's energy status. This dual approach significantly enhances the success rate of packet receptions and minimizes the occurrence of energy outages. Our simulations, conducted over a period equivalent to 1.5 years and involving more than 300 thousand receptions, utilized discrete time and energy steps to model the system's performance under various operational conditions. The results demonstrate that the strategic use of t_{wait} and t_{out}, informed by ESI feedback, can lead to substantial improvements in system performance, particularly in terms of reducing average delay times and resolving energy outages more quickly. One of the key findings is the role of battery capacity in influencing system performance. While larger battery capacities generally contribute to lower outage probabilities and shorter average delays, the benefits plateau beyond a certain point due to the diminishing returns on additional energy storage. This shows the importance of optimizing battery size based on the expected energy consumption patterns and harvesting capabilities of the system, thereby preventing the unnecessary expense associated with oversized batteries. Furthermore, the study highlights the potential drawbacks of overly cautious or conservative transmission strategies for excessive waiting times, which can lead to inefficiencies and increased average delays. The optimal balance between wait-

ing for sufficient energy accumulation and maximizing packet reception rates is crucial for achieving high system performance.

In conclusion, this thesis contributes to the ongoing development of energy-efficient communication protocols for WSNs by providing a comprehensive analysis of the factors affecting system performance. The proposed strategies, based on the use of ACKs and ESI, offer promising avenues for future research and practical implementation in real-world energy harvesting scenarios. As WSN continues to play a pivotal role in various applications, from environmental monitoring to smart cities, the insights gained from this study will be instrumental in enhancing the reliability and efficiency of these critical systems.

REFERENCES

1. Ku, M.-L., W. Li, Y. Chen, and K. J. Ray Liu, "Advances in Energy Harvesting Communications: Past, Present, and Future Challenges", *IEEE Communications Surveys & Tutorials*, Vol. 18, No. 2, pp. 1384–1412, 2016.

2. Soua, R., and P. Minet, "A Survey on Energy Efficient Techniques in Wireless Sensor Networks", *4th Joint IFIP Wireless and Mobile Networking Conference*, Toulouse, France, pp. 1–9, 2011.

3. Ma, D., G. Lan, M. Hassan, W. Hu, and S. K. Das, "Sensing, Computing, and Communications for Energy Harvesting IoTs: A Survey", *IEEE Communications Surveys & Tutorials*, Vol. 22, No. 2, pp. 1222–1250, 2020.

4. Sadowski, S., and P. Spachos, "Wireless Technologies for Smart Agricultural Monitoring Using Internet of Things Devices with Energy Harvesting Capabilities", *Computers and Electronics in Agriculture*, Vol. 172, p. 105338, 2020.

5. Sharma, H., A. Haque, and Z. A. Jaffery, "Maximization of Wireless Sensor Network Lifetime Using Solar Energy Harvesting for Smart Agriculture Monitoring", *Ad Hoc Networks*, Vol. 94, p. 101966, 2019.

6. Murphy, F. E., E. Popovici, P. Whelan, and M. Magno, "Development of a Heterogeneous Wireless Sensor Network for Instrumentation and Analysis of Beehives", *IEEE International Instrumentation and Measurement Technology Conference Proceedings*, Pisa, Italy, pp. 346–351, 2015.

7. Ochoa, I. Z., S. Gutierrez, and F. Rodríguez, "Internet of Things: Low Cost Monitoring Beehive System Using Wireless Sensor Network", *IEEE International Conference on Engineering*, Vol. 1 Veracruz, Mexico, pp. 1–7, 2019.

8. Zhang, R., A. Nayak, and J. Yu, "Sleep Scheduling in Energy Harvesting Wireless

Body Area Networks", *IEEE Communications Magazine*, Vol. 57, No. 2, pp. 95–101, 2019.

9. Hao, Y., L. Peng, H. Lu, M. M. Hassan, and A. Alamri, "Energy Harvesting Based Body Area Networks for Smart Health", *Sensors*, Vol. 17, No. 7, p. 1602, 2017.

10. Bulut, E., and I. Korpeoglu, "DSSP: A Dynamic Sleep Scheduling Protocol for Prolonging the Lifetime of Wireless Sensor Networks", *21st International Conference on Advanced Information Networking and Applications Workshops*, Vol. 2, Ontario, Canada, pp. 725–730, 2007.

11. Muzakkari, B. A., M. A. Mohamed, M. F. A. Kadir, and M. Mamat, "Queue and Priority-Aware Adaptive Duty Cycle Scheme for Energy Efficient Wireless Sensor Networks", *IEEE Access*, Vol. 8, pp. 17231–17242, 2020.

12. Chamanian, S., S. Baghaee, H. Uluşan, Zorlu, E. Uysal-Bıyıkoğlu, and H. Külah, "Implementation of Energy-Neutral Operation on Vibration Energy Harvesting WSN", *IEEE Sensors Journal*, Vol. 19, No. 8, pp. 3092–3099, 2019.

13. Guruacharya, S., V. Mittal, and E. Hossain, "Level-Triggered Harvest-Then-Consume Protocol With Two Bits or Less Energy State Information", *IEEE Wireless Communications Letters*, Vol. 7, No. 2, pp. 150–153, 2018.

14. Sharma, D., and A. P. Bhondekar, "Traffic and Energy Aware Routing for Heterogeneous Wireless Sensor Networks", *IEEE Communications Letters*, Vol. 22, No. 8, pp. 1608–1611, 2018.

15. Nguyen, T. D., J. Y. Khan, and D. T. Ngo, "A Distributed Energy-Harvesting-Aware Routing Algorithm for Heterogeneous IoT Networks", *IEEE Transactions on Green Communications and Networking*, Vol. 2, No. 4, pp. 1115–1127, 2018.

16. Zordan, D., T. Melodia, and M. Rossi, "On the Design of Temporal Compression Strategies for Energy Harvesting Sensor Networks", *IEEE Transactions on*

Wireless Communications, Vol. 15, No. 2, pp. 1336–1352, 2016.

17. Zhang, W., R. Fan, Y. Wen, and F. Liu, "Energy Optimal Wireless Data Transmission for Wearable Devices: A Compression Approach", *IEEE Transactions on Vehicular Technology*, Vol. 67, No. 10, pp. 9605–9618, 2018.

18. Hassan, M., and A. Bermak, "Solar Harvested Energy Prediction Algorithm for Wireless Sensors", *4th Asia Symposium on Quality Electronic Design*, Penang, Malaysia, pp. 178–181, 2012.

19. Castagnetti, A., A. Pegatoquet, T. N. Le, and M. Auguin, "A Joint Duty-Cycle and Transmission Power Management for Energy Harvesting WSN", *IEEE Transactions on Industrial Informatics*, Vol. 10, No. 2, pp. 928–936, 2014.

20. Ünalan, D., M. Koca, and H. Deliç, "Amplified Backscattering in RFID Communications with Energy Harvesting Tags", *International Conference on Advanced Technologies for Communications*, Ho Chi Minh City, Vietnam, pp. 21–26, 2018.

21. Demirkol, I., C. Ersoy, and E. Onur, "Wake-Up Receivers for Wireless Sensor Networks: Benefits and Challenges", *IEEE Wireless Communications*, Vol. 16, No. 4, pp. 88–96, 2009.

22. Gorlatova, M., J. Sarik, G. Grebla, M. Cong, I. Kymissis, and G. Zussman, "Movers and Shakers: Kinetic Energy Harvesting for the Internet of Things", *IEEE Journal on Selected Areas in Communications*, Vol. 33, No. 8, pp. 1624–1639, 2015.

23. Moon, K., K. M. Kim, Y. Kim, and T.-J. Lee, "Device-Selective Energy Request in RF Energy-Harvesting Networks", *IEEE Communications Letters*, Vol. 25, No. 5, pp. 1716–1719, 2021.

24. Chen, J., J. Klein, Y. Wu, S. Xing, R. Flammang, M. Heibel, and L. Zuo, "A Thermoelectric Energy Harvesting System for Powering Wireless Sensors in Nuclear Power Plants", *IEEE Transactions on Nuclear Science*, Vol. 63, No. 5, pp.

2738–2746, 2016.

25. Ko, H., S. Pack, and V. C. M. Leung, "Energy Utilization-Aware Operation Control Algorithm in Energy Harvesting Base Stations", *IEEE Internet of Things Journal*, Vol. 6, No. 6, pp. 10824–10833, 2019.

26. Farazi, S., A. G. Klein, and D. R. Brown, "Average Age of Information for Status Update Systems with an Energy Harvesting Server", *IEEE Conference on Computer Communications Workshops*, Honolulu, HI, USA, pp. 112–117, 2018.

27. Guruacharya, S., V. Mittal, and E. Hossain, "Battery Recharge Time of a Stochastic Linear and Nonlinear Energy Harvesting Systems", *IEEE Transactions on Vehicular Technology*, Vol. 67, No. 8, pp. 7877–7881, 2018.

28. Cui, S., A. Goldsmith, and A. Bahai, "Energy-Constrained Modulation Optimization", *IEEE Transactions on Wireless Communications*, Vol. 4, No. 5, pp. 2349–2360, 2005.

29. Ozel, O., and S. Ulukus, "Achieving AWGN Capacity Under Stochastic Energy Harvesting", *IEEE Transactions on Information Theory*, Vol. 58, No. 10, pp. 6471–6483, 2012.

30. Wang, Y., J. Tian, Z. Sun, L. Wang, R. Xu, M. Li and Z. Chen, "A Comprehensive Review of Battery Modeling and State Estimation Approaches for Advanced Battery Management Systems", *Renewable and Sustainable Energy Reviews*, Vol. 131, p. 110015, 2020.

31. Altinel, D., and G. Karabulut Kurt, "Energy Harvesting From Multiple RF Sources in Wireless Fading Channels", *IEEE Transactions on Vehicular Technology*, Vol. 65, No. 11, pp. 8854–8864, 2016.